VIBRATION ANALYSIS OF A CRACKED BEAM WITH ELASTIC SUPPORT

A THESIS SUBMITTED IN PARTIAL FULFILLMENT
OF THE REQUIREMENTS FOR THE DEGREE OF

Master of Technology
In
Machine Design and Analysis

By

THULASI RAM NALLA

Department of Mechanical Engineering
National Institute of Technology
Rourkela
2007

VIBRATION ANALYSIS OF A CRACKED BEAM WITH ELASTIC SUPPORT

A THESIS SUBMITTED IN PARTIAL FULFILLMENT
OF THE REQUIREMENTS FOR THE DEGREE OF

Master of Technology

In

Mechanical Engineering

By

THULASI RAM NALLA

Under the Guidance of

Prof. R.K.BEHERA

Department of Mechanical Engineering

National Institute of Technology

Rourkela

2007

National Institute of Technology

Rourkela

CERTIFICATE

This is to certify that the thesis entitled, "**Vibration Analysis of a Cracked Beam with Elastic Support**" submitted by **Sri ThulasiRam Nalla** in partial fulfillment of the requirements for the award of **Master of Technology in Mechanical Engineering** with specialization in "**Machine Design and Analysis**" at National Institute of Technology, Rourkela (Deemed University) is an authentic work carried out by him under my supervision and guidance.

To the best of my knowledge, the matter embodied in the thesis has not been submitted to any other University / Institute for the award of any Degree or Diploma.

Prof.R.K.Behera
Dept. of Mechanical Engg.
National Institute of Technology
Rourkela – 769008

Date

ACKNOWLEDGEMENT

Successful completion of work will never be one man's task. It requires hard work in right direction. There are many who have helped to make my experience as a student a rewarding one.

In particular, I express my gratitude and deep regards to my thesis guide **Prof.R.K.Behera** first for his valuable guidance, constant encouragement & kind co-operation throughout period of work which has been instrumental in the success of thesis.

I also express my sincere gratitude to **Dr. B. K. Nanda**, Head of the Department, Mechanical Engineering, for providing valuable departmental facilities.

I would like to thank my fellow post-graduate students, Mr.SadikaBaba, Mr.KrishnaSwamy and,Mr.Rajesh who made learning science a joy.

Thulasi Ram Nalla

Contents

ABSTRACT

The presences of cracks change the physical characteristics of a structure which in turn alter its dynamic response characteristics. Crack depth and location are the main parameters for the vibration analysis. So it becomes very important to monitor the changes in the response parameters of the structure to access structural integrity, performance and safety. In this current study titled “Vibration Analysis of A Cracked Beam with Elastic Support” the response characteristics of a beam is predicted for both intact and cracked beams. In addition to that the response characteristics for different crack depths are studied.

In the present study, vibration analysis is carried out on a cantilever beam with elastic support, with and without crack to study the response characteristics. Aluminum beam is used for the numerical analysis. The results obtained numerically are validated with the results obtained from the simulation. The simulations have done with the help of ANSYS software. Stability of the elastic supports for different end conditions is also analyzed under buckling load.

It is verified from both computational and simulation analysis that the presence of crack decreases the natural frequency of vibration. The mode shapes also changes considerably due to the presence of crack.

List of Tables

List of Figures

Nomenclature

a = Crack depth

B = Width of beam

D = Depth of beam

E = Young's Modulus

I = Moment of Inertia

$k_{0,} k_L$ = Extensional spring stiffness

k_T = Torsional spring stiffness

L = Undeformed length of elatic rod

P= Load

ρ = density

ξ = a/w= Relative crack depth

υ = Poisson's ratio

W = Width of beam

CHAPTER 1

INTRODUCTION

1. INTRODUCTION

The most common structural defect is the existence of a crack. Cracks are present in structures due to various reasons. The presence of a crack could not only cause a local variation in the stiffness but it could affect the mechanical behavior of the entire structure to a considerable extent.

In early 1970s the dynamic response of cracked beams and rotors has been investigated increasingly because damages in rotating shaft of various power transmissions occurred quite often. Cracks may be caused by fatigue under service conditions as a result of the limited fatigue strength. They may also occur due to mechanical defects. Another group of cracks are initiated during the manufacturing processes. Generally they are small in sizes. Such small cracks are known to propagate due to fluctuating stress conditions. If these propagating cracks remain undetected and reach their critical size, then a sudden structural failure may occur.

If a structure is defective, there is a change in the stiffness and damping of the structure in the region of the defect. Usually, stiffness decreases and damping increases if the defect appears in the form of a micro or macro crack. A reduction in stiffness implies a reduction in the natural frequencies of vibration. A crack on a structural member introduces a local flexibility which is a function of the crack depth. Major characteristics of structures, which undergo change due to presence of crack, are

- The natural frequency
- The amplitude response due to vibration
- Mode shape.

Hence it is possible to use natural frequency measurements to detect cracks.

The objective is to carry out vibration analysis on a cantilever beam with elastic support with and without crack. The results obtained analytically are validated with the simulation results. Stability of the elastic supports for different end conditions is also analyzed under buckling load.

CHAPTER 2

LITERATURE REVIEW

2. LITERATURE REVIEW

For vibrational analysis of cracked beams and possible crack detection, the fracture mechanics procedure is generally preferred. According to this procedure the crack occurring in a beam would reduce the local stiffness at the location of crack. In using the fracture mechanics model, the local stiffness at the crack section is calculated using Castigliano's second theorem as applicable to fracture mechanics formulations. The calculated local stiffness is then modeled by a flexural spring for the bending vibration of a cracked beam. To establish the vibration equations, the cracked is represented by two structures connected by flexural spring.

Irwin [1,2], A crack on an elastic structural element introduces considerable local flexibility due to the strain energy concentration in the vicinity of the crack tip under load. This effect has been recognized long ago. A local compliance has been used to quantify, in a microscopic way, the relation between the applied load and the strain energy concentration around the tip of the crack.

Krawczuk and ostachowicz [3,4,5] have analyzed the effect of positions and depth of two cracks on the natural frequencies of a cantilever beam and shaft. A finite element methods has been used for modeling the cracked beam and has proposed that finite element method can be used for cracked rotor analysis.

Dimarogonas [6, 7] has noticed that for small cr4ack depths the decrease in natural frequency is proportional to the square of crack depth ratio.

Matvev et al. [8] expressions for bending vibrations of an Euler-Bernoulli cracked beam have been analyzed. They have studied the effects of the ratio of crack location to the length of the beam and also ratio of depth of the crack to the height of the beam. They have investigated the variation of the natural frequency of the cracked beam.

Adams et al. [9] have studied a free-free bar with localized damage. The damage has been modeled by a linear spring of infinitesimal length separating two sections of the bar. They have shown analytical and experimental results for natural frequencies of longitudinal vibration.

Springer et al. [10] have examined the free longitudinal vibration of a bar with free ends and two cracks located symmetrically at the centre of the span. The cracks have been modeled in two ways. One is using linear springs, the other is using reductions in cross-sectional area. The changes in natural frequencies are close to those obtained from experiments.

Krawczuk and Ostachowicz [11,12] have investigated the effect of the longitudinal static loads on lateral vibrations of beams.

Silva and Gomez [13-15] have performed an extensive experimental dynamic analysis for the prediction of the location and the depth of cracks in straight beams. They have described the experimental techniques and presented the results obtained for various locations and depths of crack.

Chondros et al. [16] have analyzed the lateral vibration of cracked Euler-Bernoulli beams with single or double edge cracks. Their analysis can be used for the prediction of the dynamic response of a simply supported beam with open surface cracks.

Papadopoulos [17] has studied the torsional vibrations of rotors with transverse surface crack. The crack has been modelled by way of a local flexibility matrix which was subsequently calculated analytically and measured experimentally. A good agreement has been obtained between the theoretical and experimental results.

Pandey et al. [18] have reported the changes in mode shapes due to presence of crack in structures.

Qian et al.[19] have used a finite element model to analyze the effect of crack closure on the transverse vibration of a beam. The stiffness matrix of the system has been deduced from the stress intensity factors, and it gives two values, one for the close crack (uncracked beam) and for the other for the open crack. The sign of the stress on the crack faces has been used to determine if the crack is open or closed at each time step.

Zheng and Fan[20] have presented a modified Fourier Series (MFS) method for computing the natural frequencies of a non-uniform with an arbitrary number of transverse open cracks.Based on modified Fourier series, one can treat the cracked beam in the most usual way and thus reduce the problem to a simple one.

Timoshenko and Gere [21] have obtained the exact solutions to the non-linear differential equations governing large deformations of an elastic rod only in cases of very simple loading and boundary conditions, such as end-loaded, fixed-free or simply supported columns. By necessity, approximate solution techniques have been employed for problems involving more general loads and supports.

Wang [22] have utilized a power series expansion method to study the postbuckling of a column under a distributed axial load. In the classical analysis of buckling of columns, the deflection is assumed small and the square of their derivatives is neglected. The differential equation based upon the approximate expression of curvature has been used in calculating buckling load. Results from this kind of calculation gives the buckling load at which the lateral deflection of column is indeterminate and unbounded. Wang [23, 24] have pointed out the limitations of power series methods.

Tauchert and Lu [25] have utilized an energy approach to investigate the postbuckling of an initially deformed, simply supported rod. In actual case, however, the column will have finite and determinate deflection at the critical load. Such paradoxical result is due to the fact that the approximate theory is used in the analysis. A simple variation of the well-known method of minimizing a function of several variables by changing one parameter at a time is described. This variation is such that when the procedure is applied to a quadratic form, it causes conjugate directions to be chosen, so the ultimate rate of

convergence is fast when the method and it ensures that the convergence rate from a bad approximation to a minimum is always efficient. Practical applications of the procedure have proved to the very satisfactory, and numerical examples are given in which functions of up to twenty variables are minimized. The method finds an unconstrained minimum of a function of several variables without calculating derivatives. The examples presented and the theory behind the method suggests that it is significantly more efficient than other methods which have been referred to, but it does contain two unsatisfactory features. The first is that as the number of variables increases there is a tendency for new directions to be chosen less often. This could be overcome by always using a new direction and forcing the remaining directions to be conjugate to than new one by a projection technique, but this would require each iteration to demand approximately three times as many function values. The ultimate convergence criterion is also unsatisfactory, but it is not an essential part of the method and any improved criterion could easily incorporated.

Wilson and Snyder [26] have numerically integrated the equations governing the finite deformation of an elastic cantilever beam with a tip payload and an eccentric tip follower load. A high flexure manipulator arm is modeled as a cantilever beam with a tip payload and an eccentric tip follower load that drives the arm. The shapes of the resulting elastic curves for finite deformations (the elastica) are calculated in terms of nondimensional system parameters. For critical combinations of these parameters, a small increment in the driving follower load causes an abrupt change in the shape of elastica. The abrupt change in tip angle is typically of the order of $\prod$ radians. These results are applicable to the design of high flexure robotic manipulators.

Dimarogonas, et al. [27] have computed the flexibility matrix for a transverse surface crack for a shaft subjected to bending.

Chondros, et al. [28] have combined the spring hinge model with fracture mechanics results, and developed a frequency spectral method to identify cracks in various structures. For a known crack position this method correlated the crack depth to the changes in natural frequencies of the first three modes.

Dimarogonas, et al. [29] have studied the influence of a circumferential crack upon the torsional dynamic behavior of a shaft. They have found that due to the presence of crack, the torsional natural frequencies decreases due to the added flexibility. The strain energy release function is related to the compliance of the cracked shaft due to the introduction of a crack.

Rizos, et al. [30] have determined the crack location and its depth in a cantilever beam from the vibration modes. They achieved this by measuring the flexural vibrations of a cantilever beam with rectangular cross-section with a transverse surface crack. Analytical results are used to relate the measured vibration modes to the crack location and depth. From the measured amplitudes at two points of the structure vibrating at one of its natural modes, the respective vibration frequency and an analytical solution of the dynamic response, the crack location can be found and depth can be estimated with satisfactory accuracy

Mermertas, et al. [31] have studied the effect of mass attachment on the transverse vibration characteristics of a cracked cantilever beam. Investigation of the cracked beam has been carried out theoretically. The governing equation for free vibrations of the cracked beam is constructed from the Bernoulli-Euler beam elements. To model the transverse vibration, the crack is represented by a rotational spring. The relative changes of the first three natural frequencies as a function of the location of the attached mass are presented. The crack was located in two different distances from the fixed end of the beam. The results for the changes of the natural frequencies of a cracked beam carrying a point mass are compared with the results of the beam without a crack.

Bamnios, et al. [32] have investigated the influence of the transverse surface crack on the dynamic behavior of cantilever beam both analytically and experimentally. They have modeled the crack as rotational spring and related the change in natural frequency and mechanical impedance to the location and crack depth.

Nahvi, et al. [33] have developed an analytical and experimental approach for crack detection in cantilever beams by vibration analysis. To avoid non-linearity, it is assumed that the crack is always open. To identify the crack, contours of the normalized frequency in terms of the normalized crack depth and location are plotted. The intersection of contours with the constant modal natural frequency planes is used to relate the crack location and depth. A minimization approach is employed for identifying the cracked element within the cantilever beam.

Chandra Kishen, et al. [34] have studied the fracture behavior of cracked beams and columns using finite element analysis. Assuming that failure occurs due to crack propagation when the mode I stress intensity factor reaches the fracture toughness of the material, the failure load of cracked columns are determined for different crack depths and slenderness ratios.

Krawczuk, et al. [35] formulated a cracked beam finite element based on Elastic - plastic fracture mechanics and finite element method. Crack tip plasticity, at the cracked cross-section, is included in the model of local flexibility. The inertia and stiffness matrices take into account the effect of flexural bending deformation due to the crack presence.

Octachowitz et al [36] presented a method for analysis of the effect of two open cracks upon the frequencies of the natural flexural vibration in a cantilever beam. Two types of cracks are considered: double-sided, occurring in the case of cyclic loadings, and single-sided crack, which in principle occurs as a result of fluctuating loadings. It is also assumed that the cracks occur in the first mode fracture i.e. the opening mode. It is concluded that in the case of two cracks of different depths, the larger crack has the most significant effect on natural vibration frequencies. It is also concluded that double-sided cracks affect the vibration frequencies to a smaller degree than single cracks with same relative depth of crack and the same position.

Behera [37] in his research work has developed the theoretical expressions to find out the natural frequencies and mode shapes for the cantilever beam with single crack. Experiments have been conducted to prove the authenticity of the theory developed.

Parhi [38] has studied the dynamic behavior of a beam/rotor structures with transverse crack subjected to external force. He has investigated the dynamic response of structures subjected to moving mass and dynamic response of rotors in viscous fluids with a single crack. Experiments have been conducted, and compared with theoretical results. He found that there is a change in the mode shapes with crack.

CHAPTER 3

CRACK THEORY

3. CRACK THEORY

3.1 Regimes of a cracked body

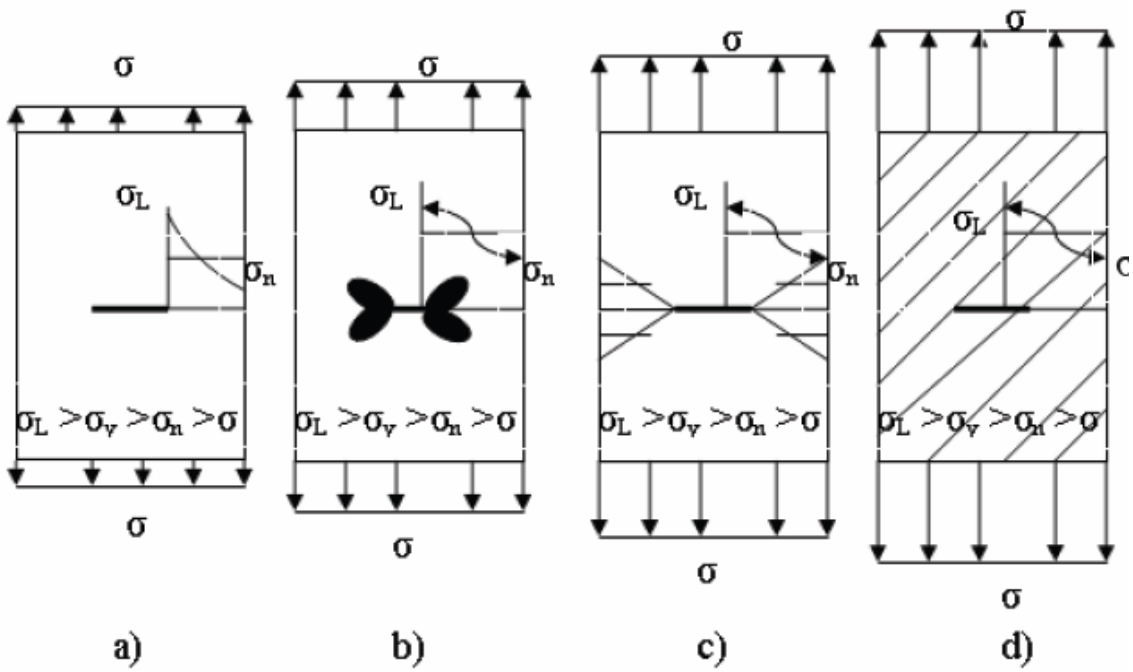

Figure 3.1 Regimes of a cracked body

Figure shows the four different regimes that a cracked body can experience depending on the toughness of the material. The arrows at the end of the specimen depict the magnitude of loading. The extent of plastic zone is represented by the black or shaded area. Brief descriptions of the four regimes are given below.

Here σ is the applied stress, σ_y is the yield stress, σ_n is the normal stress,

- **Linear Elastic Fracture Mechanics (LEFM) regime**. Yielding is limited to a very small zone in the immediate vicinity of the crack tip (small scale yielding).
- **Elastic-Plastic regime.** A yield zone develops ahead of the crack tip but yielding remains unconstrained, i.e., the plastic zone does not reach the lateral boundary of the structure.
- **Gross yield (or the net section yield)**: - Yielding spreads to the lateral boundaries and become uncontained. Failure may be due to fast unstable crack propagation, by plastic collapse of the net section, or by stable tearing followed by tearing in stability.

• **General yielding: -** The applied stress is larger than the yield stress. The whole structure is plasticized. Plastic collapse and tearing instability are the dominant failure modes.

Limitations of LEFM: - The LEFM solutions for crack tip stress fields predict infinite stresses at the tip. Since real materials yield at a finite stress, the LEFM solutions lose their validity in the immediate vicinity of the crack tip. However according to McClintock and Irwin, the basic assumptions of fracture mechanics remain valid if the yielding is confined to a very small plastic zone at the crack tip surround by a elastic region in which the crack tip stress field is governing the stress distribution.

3.2 Modes of Fracture: -The three basic types of loading that a crack experiences are

• **Mode I** corresponds to the opening mode in which the crack faces separates in a direction normal to the plane of the crack and the corresponding displacements of crack walls are symmetric with respect to the crack front. Loading is normal to the crack plane, and tends to open the crack. Mode I is generally considered the most dangerous loading situation.

• **Mode II** corresponds to in-plane shear loading and tends to slide one crack face with respect to the other (shearing mode). The stress is parallel to the crack growth direction.

• **Mode III** corresponds to out-of-plane shear, or tearing. In which the crack faces are sheared parallel to the crack front.

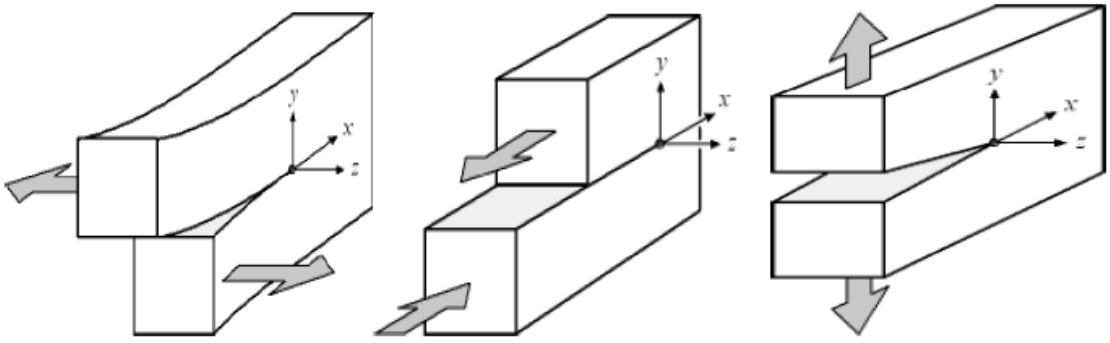

Figure 3.2 Three basic modes of fracture

3.3 Stress Intensity Factor (SIF), K: - It is defined as a measure of the stress field intensity near the tip of an ideal crack in a linear elastic solid when the crack surfaces are displaced in the opening mode (Mode I). (SIFs) are used to define the magnitude of the singular stress and displacement fields (local stresses and displacements near the crack tip). The SIF depends on the loading, the crack size, the crack shape, and the geometric boundaries of the specimen. The recommended units for K are MPa√m. it is customary to write the general formula in the form $K=Y\sigma\sqrt{\pi a}$ where σ is the applied stress, a is crack depth, Y is dimensionless shape factor.

3.4 Physical parameters affecting Dynamic characteristics of cracked structures:

Usually the physical dimensions, boundary conditions, the material properties of the structure play important role for the determination of its dynamic response. Their vibrations cause changes in dynamic characteristics of structures. In addition to this presence of a crack in structures modifies its dynamic behavior. The following aspects of the crack greatly influence the dynamic response of the structure.

(i) The position of crack

(ii) The depth of crack

(iii) The orientation of crack

(iv) The number of cracks

3.5 Classification of cracks

Based on their geometries, cracks can be broadly classified as follows:

- Cracks perpendicular to the beam axis are known as “transverse cracks”. These are the most common and most serious as they reduce the cross-section and thereby weaken the beam. They introduce a local flexibility in the stiffness of the beam due to strain energy concentration in the vicinity of the crack tip.
- Cracks parallel to the beam axis are known as “longitudinal cracks”. They are not that common but they pose danger when the tensile load is applied is at right angles to the crack direction i.e. perpendicular to beam axis or the perpendicular to crack.

• "Slant cracks" (cracks at an angle to the beam axis) are also encountered, but are not very common. These influence the torsion behavior of the beam. Their effect on lateral vibrations is less than that of transverse cracks of comparable severity.

• Cracks that open when the affected part of the material is subjected to tensile stresses and close when the stress is reversed are known as "breathing cracks". The stiffness of the component is most influenced when under tension. The breathing of the crack results in non-linearity's in the vibration behavior of the beam. Cracks breathe when crack sizes are small, running speeds are low and radial forces are large .Most theoretical research efforts are concentrated on "transverse breathing" cracks due to their direct practical relevance.

• Cracks that always remain open are known as "gaping cracks". They are more correctly called "notches". Gaping cracks are easy to mimic in a laboratory environment and hence most experimental work is focused on this particular crack type.

• Cracks that open on the surface are called "surface cracks". They can normally be detected by techniques such as dye-penetrates or visual inspection.

• Cracks that do not show on the surface are called "subsurface cracks". Special techniques such as ultrasonic, magnetic particle, radiography or shaft voltage drop are needed to detect them. Surface cracks have a greater effect than subsurface cracks on the vibration behavior of shafts.

3.6 Crack Propagation

In 1920, Griffith formulated the concept that a crack in an ideally brittle component will propagate if the total energy of the system is lowered with crack propagation. In other words, if the change in elastic strain energy due to crack extension is larger than the energy required to create new crack surfaces, the crack will propagate. The Griffith theory in equation form is:

$$\frac{dP}{da} \geq \frac{d(W_s)}{da} \qquad (3.6.1)$$

Where a is the crack depth, Ws is the work done by external forces per unit thickness, and P is the potential energy supplied by the internal strain energy and external forces. The crack will propagate if $-\frac{dp}{da}$ is greater than or equal to $\frac{dW_s}{da}$

In 1949, Irwin extended Griffith's theory to ductile materials by including the energy dissipated by local plastic flow. He postulated that the energy due to plastic deformation must be added to the surface energy associated with the creation of new crack surfaces. For ductile materials, the surface energy term is often negligible compared to the energy associated with plastic deformation. In 1956, Irwin defined a new quantity, G, the strain energy release rate (also called the crack extension force or the crack driving force). The strain energy release rate for a linear elastic material is defined as the total energy absorbed during cracking per unit increase in the crack length and per unit thickness. The crack will propagate when a critical strain energy release rate, Gc, is achieved (when G is greater than or equal to the crack resistance energy, Gc). The equation below shows Irwin's modification to the Griffith theory, where U is the strain energy stored in the body per unit thickness.

$$G = -\frac{dP}{da} = \frac{d(W_s)}{da} = -\frac{dU}{da} \qquad (3.6.2)$$

CHAPTER 4

PROBLEM

4. PROBLEM

4.1 PROBLEM DEFINITION

The problem involves calculation of natural frequencies and mode shapes for cantilever beam with elastic support without a crack and with single crack of different crack depths. The results calculated analytically are validated with the results obtained by simulation analysis.

Stability of the elastic supports for different end conditions is also analyzed under buckling load.

4.2 FREQENCY ANALYSIS OF BEAM WITHOUT CRACK SUPPORTED BY ELASTIC SUPPORTS

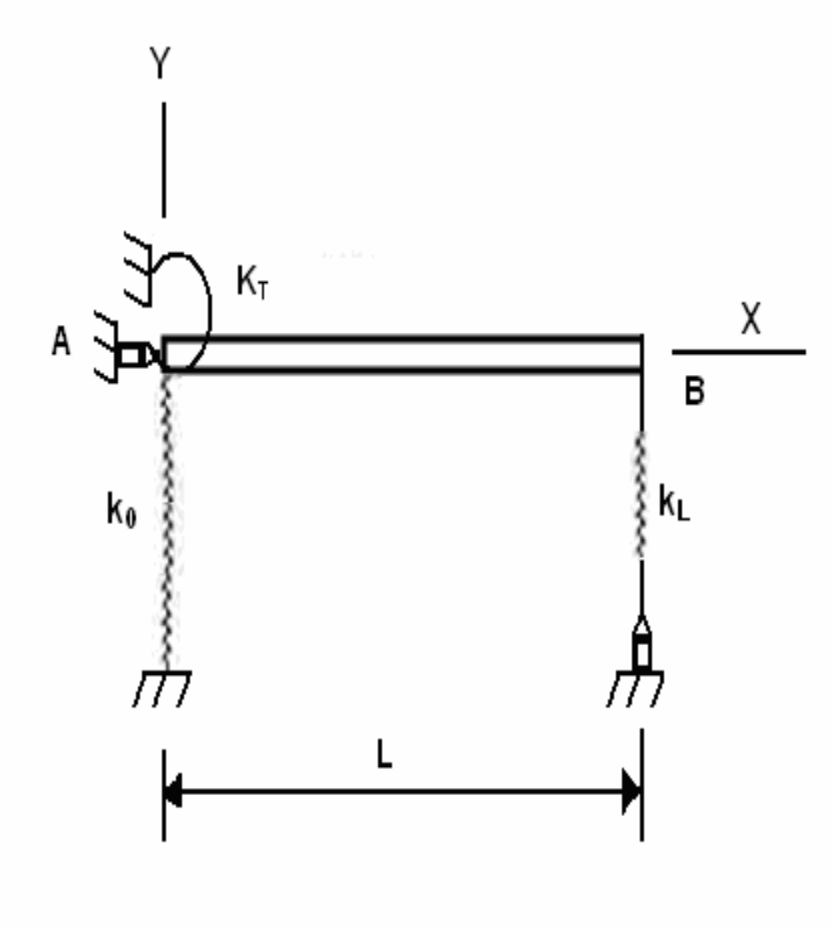

Figure 4.2.1 Beam with elastic support

A slender, elastic rod of undeformed length L, elastically supported by extensional springs having stiffness k_0, and k_L, and a torsional spring of stiffness k_T,as shown in Fig.

Boundary conditions for beam:

$$-k_0 w(0) = EI\frac{d^3 w(0)}{dx^3} \tag{4.1}$$

$$k_L w(L) = EI\frac{d^3 w(L)}{dx^3} \tag{4.2}$$

$$k_T \frac{dw(0)}{dx} = EI\frac{d^2 w(0)}{dx^2} \tag{4.3}$$

$$0 = EI\frac{d^2 w(L)}{dx^2} \tag{4.4}$$

The displacements of the beam is

$$Y(\beta) = A_1\cos(\lambda\beta) + A_2\sin(\lambda\beta) + A_3\cosh(\lambda\beta) + A_4\sinh(\lambda\beta).....(3) \tag{4.5}$$

λ and β are non dimensional parameter given by $\lambda^4 = \frac{\omega^2 \rho A L^4}{EI}, \beta = \frac{x}{L}$ (4.6)

The normal function coefficients of matrix are obtained from equation (4.5) using boundary conditions given by equations (4.1-4.4).The obtained system matrix is

$$\begin{bmatrix} -k_0^* & -\lambda^3 & -k_0^* & -\lambda^3 \\ k_L^*\cos\lambda - \lambda^3\sin\lambda & k_L^*\sin\lambda + \lambda^3\cos\lambda & k_L^*\cosh\lambda - \lambda^3\sinh\lambda & k_L^*\sinh\lambda - \lambda^3\cosh\lambda \\ \lambda & k_T^* & -\lambda & k_T^* \\ -\frac{EI\lambda^2}{L^2}\cos\lambda & -\frac{EI\lambda^2}{L^2}\sin\lambda & \frac{EI\lambda^2}{L^2}\cosh\lambda & \frac{EI\lambda^2}{L^2}\sinh\lambda \end{bmatrix} \begin{bmatrix} A_1 \\ A_2 \\ A_3 \\ A_4 \end{bmatrix} = 0$$

$$k_0^* = \frac{k_0 L^3}{EI}, k_L^* = \frac{k_L L^3}{EI}, k_T^* = \frac{k_T L}{EI}$$

Where x is the coordinate along the beam, L is the length of the beam, ω is the natural angular frequency.

Aluminum has taken the beam. The properties of the Aluminum

Density of Aluminum=2.77 gm/cm^3

Young's modulus of Aluminum=0.724e12 dynes/cm^2

Poisson's ratio=0.3

Width of beam (B) =5 cm

Length of beam (L) =80 cm

Depth of beam (D) =0.6 cm

I=Moment of inertia i.e. $\frac{BD^3}{12}$

K_0=stiffness of linear spring at x=0 is taken as 1e44 dynes/cm

K_L=stiffness of linear spring at x=L is taken as zero.

K_T=stiffness of torsional spring is taken as 1e44 dynes/cm

The natural frequencies of the beam are found out by equating the determinant of coefficient matrix is zero. The equation is satisfied for an infinite number of system's natural frequencies.

$$\begin{vmatrix} -k_0^* & -\lambda^3 & -k_0^* & -\lambda^3 \\ k_L^*\cos\lambda - \lambda^3\sin\lambda & k_L^*\sin\lambda + \lambda^3\cos\lambda & k_L^*\cosh\lambda - \lambda^3\sinh\lambda & k_L^*\sinh\lambda - \lambda^3\cosh\lambda \\ \lambda & k_T^* & -\lambda & k_T^* \\ -\frac{EI\lambda^2}{L^2}\cos\lambda & -\frac{EI\lambda^2}{L^2}\sin\lambda & \frac{EI\lambda^2}{L^2}\cosh\lambda & \frac{EI\lambda^2}{L^2}\sinh\lambda \end{vmatrix} = 0$$

4.3 BEAM WITH SINGLE CRACK:

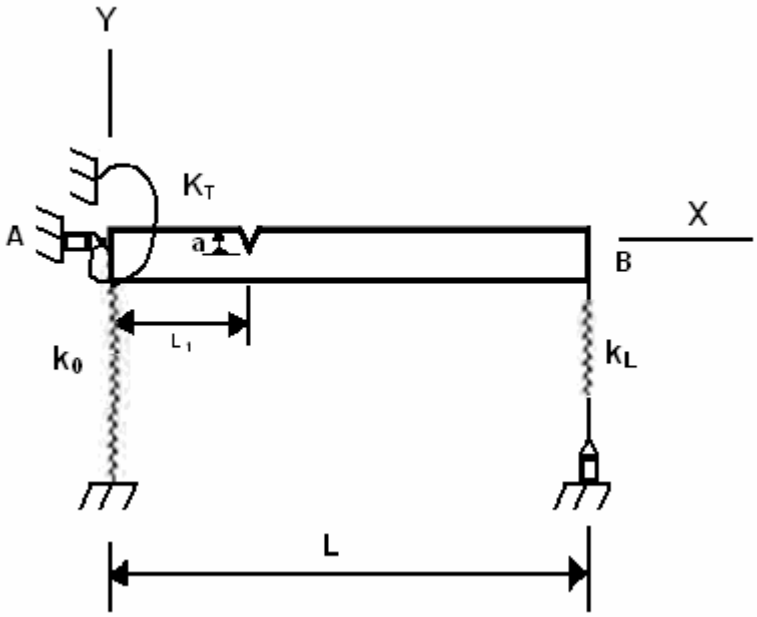

Figure 4.3.1 Single cracked beam with elastic support

The location of the crack divides beam into two parts as shown in fig. The bending displacements in the regions left and right of the crack are denoted as $w_1(x)$,$w_2(x)$. The continuity of deflection, bending moment, shear force is given by

$$w_1(\beta_c) = w_2(\beta_c) \tag{4.7}$$

$$w_1''(\beta_c) = w_2''(\beta_c) \tag{4.8}$$

$$w_1'''(\beta_c) = w_2'''(\beta_c) \tag{4.9}$$

$$m_3 m_4 w_1''(\beta_c) = m_4[w_2'(\beta_c) - w_1'(\beta_c)] \tag{4.10}$$

$$\left[m_3 = \frac{EI}{Lk_{22}}, m_4 = \frac{EI}{L^2 k_{21}}, \beta_c = \frac{L_1}{L} \right]$$

The boundary conditions for the beam

$$-k_0 w(0) = EI \frac{d^3 w(0)}{dx^3} \tag{4.11}$$

$$k_L w(L) = EI \frac{d^3 w(L)}{dx^3} \tag{4.12}$$

$$k_T \frac{dw(0)}{dx} = EI \frac{d^2 w(0)}{dx^2} \tag{4.13}$$

$$0 = EI \frac{d^2 w(L)}{dx^2} \tag{4.14}$$

The displacements on each part of the beam

$$Y_1(\beta) = A_1 \cos(\lambda\beta) + A_2 \sin(\lambda\beta) + A_3 \cosh(\lambda\beta) + A_4 \sinh(\lambda\beta) \tag{4.15}$$

$$Y_2(\beta) = A_5 \cos(\lambda\beta) + A_6 \sin(\lambda\beta) + A_7 \cosh(\lambda\beta) + A_8 \sinh(\lambda\beta) \tag{4.16}$$

λ and β are nondimensional parameter given by $\lambda^4 = \frac{\omega^2 \rho A L^4}{EI}, \beta = \frac{x}{L}$

$$\begin{bmatrix}
-k_0^* & \lambda^3 & -k_0^* & \lambda^3 \\
k_L^* \cos\lambda - \lambda^3 \sin\lambda & k_L^* \sin\lambda + \lambda^3 \cos\lambda & k_L^* \cosh\lambda - \lambda^3 \sinh\lambda & k_L^* \sinh\lambda - \lambda^3 \cosh\lambda \\
\lambda & k_T^* & -\lambda & k_T^* \\
-\frac{EI\lambda^2 \cos\lambda}{L^2} & -\frac{EI\lambda^2 \sin\lambda}{L^2} & \frac{EI\lambda^2 \cosh\lambda}{L^2} & \frac{EI\lambda^2 \sinh\lambda}{L^2} \\
\cos\lambda\beta & \sin\lambda\beta & \cosh\lambda\beta & \sinh\lambda\beta \\
-\lambda^2 \cos\lambda\beta & -\lambda^2 \sin\lambda\beta & \lambda^2 \cosh\lambda\beta & \lambda^2 \sinh\lambda\beta \\
\lambda^3 \sin\lambda\beta & -\lambda^3 \cos\lambda\beta & \lambda^3 \sinh\lambda\beta & \lambda^3 \cosh\lambda\beta \\
-m_3\lambda \cos\lambda\beta - \sin\lambda\beta & -m_3\lambda \sin\lambda\beta + \cos\lambda\beta & m_3\lambda \cosh\lambda\beta + \sinh\lambda\beta & m_3\lambda \sinh\lambda\beta + \cosh\lambda\beta
\end{bmatrix}$$

$$\begin{bmatrix}
0 & 0 & 0 & 0 \\
0 & 0 & 0 & 0 \\
0 & 0 & 0 & 0 \\
0 & 0 & 0 & 0 \\
-\cos\lambda\beta & -\sin\lambda\beta & -\cosh\lambda\beta & -\sinh\lambda\beta \\
\lambda^2 \cos\lambda\beta & \lambda^2 \sin\lambda\beta & -\lambda^2 \cosh\lambda\beta & -\lambda^2 \sinh\lambda\beta \\
-\lambda^3 \sin\lambda\beta & \lambda^3 \cos\lambda\beta & -\lambda^3 \sinh\lambda\beta & -\lambda^3 \cosh\lambda\beta \\
\sin\lambda\beta & -\cos\lambda\beta & -\sinh\lambda\beta & -\cosh\lambda\beta
\end{bmatrix}
\begin{bmatrix} A_1 \\ A_2 \\ A_3 \\ A_4 \\ A_5 \\ A_6 \\ A_7 \\ A_8 \end{bmatrix} = 0 \tag{4.17}$$

The normal function coefficients of matrix are obtained from the equation (4.15) and (4.16) using the boundary conditions given by equations (4.7-4.14). The system matrix is given in equation (4.17). The natural frequencies of the cracked beam are found out by equating the determinant of coefficient matrix to zero. The equation (4.17) is satisfied for

an infinite number of system's natural frequencies. Knowing the natural frequency and setting A_1=1, the other values A_2 to A_8 are found out.

Where A_i for i = 1…8 are normal function constant. Substituting any one of these back into equations (4.15) and (4.16) yields a corresponding set of relative values for A_1 to A_8 they are called mode shapes corresponding to the natural frequency.

The influence coefficients are calculated as follows.

$$C_{11} = \frac{2\pi}{BE'}\int_0^{\xi_1} \xi\left[F_1(\xi)\right]^2 d\xi$$

$$C_{12} = C_{21} = \frac{12\pi}{E'BW}\int_0^{\xi_1} \xi[F_1(\xi)F_2(\xi)]d\xi$$

$$C_{22} = \frac{72\pi}{E'BW^2}\int_0^{\xi_1} \xi[F_2(\xi)]^2 d\xi$$

where $\xi = \frac{a}{W}\,(\text{Relativecrack depth})$ and $E' = \frac{E}{1-\upsilon^2}$

The functions F_1 and F_2 are dependent on the crack depth 'a' and are approximated by

$$F_1\left(\frac{a}{w}\right) = \left[\frac{2w}{\pi a}\tan\left(\frac{\pi a}{2w}\right)\right]^{0.5}\left\{\frac{0.752 + 2.02\left(a/w\right) + 0.37\left[1-\sin\left(\pi a/2w\right)\right]^3}{\cos\left(\pi a/2w\right)}\right\}$$

$$F_2\left(\frac{a}{w}\right) = \left[\frac{2w}{\pi a}\tan\left(\frac{\pi a}{2w}\right)\right]^{0.5}\left\{\frac{0.923 + 0.199\left[1-\sin\left(\pi a/2w\right)\right]^4}{\cos\left(\pi a/2w\right)}\right\}$$

The stiffness matrix for the cracked beam is obtained as

$$K = \begin{bmatrix} K_{11} & K_{12} \\ K_{21} & K_{22} \end{bmatrix} = \begin{bmatrix} C_{11} & C_{12} \\ C_{21} & C_{22} \end{bmatrix}^{-1}$$

4.4. METHOD OF ANALYSIS:

Consider a slender, elastic beam of undeformed length L, elastically supported by extensional springs having stiffness $k_{0,}$ and k_L, and a torsional spring of stiffness k_T, as shown in fig. 4.4.1. The beam is subjected to an end-load P.

The radius of curvature, slope, and the displacement components in the x and y directions are denoted by $\rho, \theta(s), u(s), w(s)$, respectively (Fig.4.4.2). Here s is the arc length along the beam centerline. Neglecting the strain energy associated with axial and shear deformation, the strain energy U_R for an initially straight beam may be expressed as

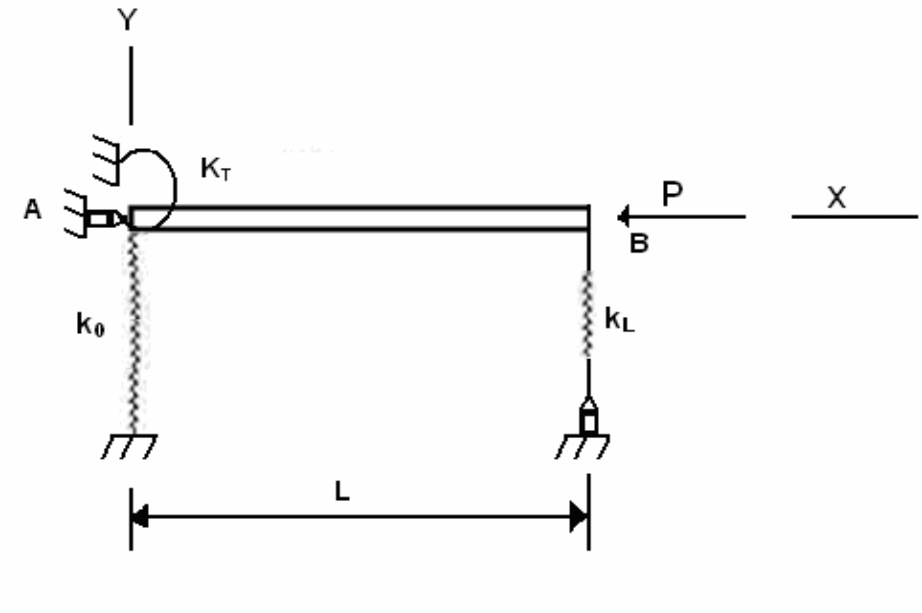

Fig.4.4.1 Loading and support conditions for elastic beam

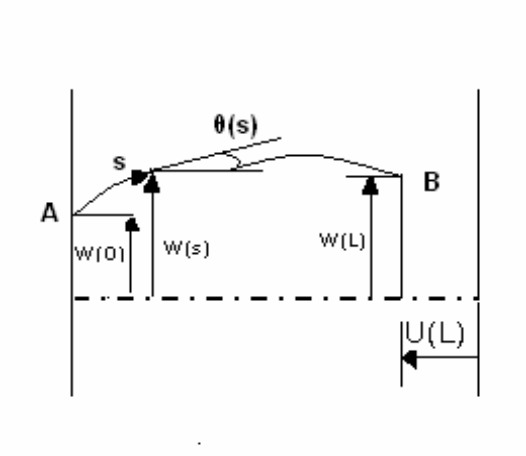

Figure 4.4.2 deformation of beam

Where EI is the bending stiffness of the beam.

$$du = \int \frac{\sigma^2}{2E} * \text{volume}$$

$$du = \int \frac{M^2 y^2}{2EI^2} dx dA$$

$$du = \frac{M^2 dx}{2EI^2} \int y^2 dA$$

$$du = \frac{M^2 dx}{2EI^2} I$$

$$du = \frac{M^2}{2EI} dx$$

$$du = \frac{M^2}{2EI} ds$$

$$U = \int_0^L \frac{M^2}{2EI} ds$$

$$\frac{M}{EI} = \frac{1}{R} = \frac{d^2 y}{dx^2}$$

$$U = \int_0^L \left(\frac{EI}{R}\right)^2 \frac{1}{2EI} ds$$

$$U = \int_0^L \left(\frac{EI}{2}\right)\left(\frac{1}{R}\right)^2 ds$$

$$U_R = \int_0^L \frac{EI}{2}\left(\frac{1}{\rho}\right)^2 ds$$

An exact expression for the curvature

$$\frac{1}{\rho} = \frac{d\theta}{ds}$$

$$\sin\theta = \frac{dw}{ds}$$

$$\theta = \sin^{-1}\left(\frac{dw}{ds}\right)$$

$$\frac{d\theta}{ds} = \frac{d^2w/dx^2}{\sqrt{1-\left(\frac{dw}{dx}\right)^2}}$$

$$\frac{1}{\rho} = \frac{d\theta}{ds} = \frac{d^2w/dx^2}{\sqrt{1-\left(\frac{dw}{dx}\right)^2}}$$

The strain energy U_S of the linear spring is

$$U_s = \frac{1}{2}k_0[w(0)]^2 + \frac{1}{2}k_L[w(L)]^2 + \frac{1}{2}k_T[\theta(0)]^2$$

Where w(L), $\theta(0)$ can be expressed as

$$dw = \sin\theta ds$$

$$\int_0^L dw = \int_0^L \sin\theta ds$$

$$w(L) - w(0) = \int_0^L \sin\theta ds$$

$$w(L) = \int_0^L \sin\theta ds + w(0)$$

Potential energy VP=force*displacement

VP=p*u (L)

Where u(L) denotes the displacement in the x direction at the end of the rod. Assuming rod is inextensible, u(L) can be expressed as

$$-u(L) = L - \int_0^L \cos\theta ds$$

$$\sin\theta = \frac{dw}{ds}$$

$$\cos\theta = \sqrt{1-\sin^2\theta}$$

$$-u(L) = L - \int_0^L \sqrt{1-\left(\frac{dw}{ds}\right)^2}\, ds$$

Thus the total potential energy $\Pi = U_R + U_S + V_P$ of the system, written in terms of the transverse displacement w(s), is given by

$$\Pi = \int_0^L \frac{EI}{2}\left[\frac{d^2w/ds^2}{\sqrt{1-\left(\frac{dw}{ds}\right)^2}}\right]^2 ds + \frac{1}{2}k_0[w(0)]^2 + \frac{1}{2}k_L[w(L)]^2$$

$$+\frac{1}{2}k_T\left[\sin^{-1}\left(\frac{dw(0)}{ds}\right)\right]^2 - P\left[L - \int_0^L \sqrt{1-\left(\frac{dw}{ds}\right)^2}\, ds\right]$$

Where expressed in terms of the slope $\theta(s)$ rather than $w(s)$ the total potential energy becomes

$$\Pi = \int_0^L \frac{EI}{2}\left(\frac{d\theta}{ds}\right)^2 ds + \frac{1}{2}k_0[w(0)]^2 + \frac{1}{2}\left[\int_0^L \sin\theta ds + w(0)\right]^2 + \frac{1}{2}k_T[\theta(0)]^2 - p\left[L - \int_0^L \cos\theta ds\right]$$

4.5 STABILITY BOUNDARIES:

Stability loads for the elastically supported beam as shown in Fig (4.4.1). can be obtained by finding non-trival solutions to the corresponding linearized problem. The linearized differential equation is

$$\frac{d^4y}{dx^4} + \beta^2\frac{d^2w}{dx^4} = 0, \beta^2 = \frac{p}{EI} \qquad (4.18)$$

And the associated boundary conditions are

$$-k_0 w(0) = EI\frac{d^3w(0)}{dx^3} + p\frac{dw(0)}{dx} \qquad (4.19)$$

$$k_L w(L) = EI\frac{d^3w(L)}{dx^3} + p\frac{dw(L)}{dx} \qquad (4.20)$$

$$k_T \frac{dw(0)}{dx} = EI \frac{d^2 w(0)}{dx^2} \tag{4.21}$$

$$0 = EI \frac{d^2 w(L)}{dx^2} \tag{4.22}$$

For convenience in analysis the following non-dimensional quantities are introduced.

$$k_0^* = \frac{k_0 L^3}{EI}, k_L^* = \frac{k_L L^3}{EI}, k_T^* = \frac{k_T L}{EI}, \Omega = \beta L, p^* = \frac{PL^2}{EI} \tag{4.23}$$

Non-trival solutions of the above equations correspond to the roots of the characteristic equation

$$\begin{aligned} &-k_0^* k_L^* k_T^* \Omega \cos\Omega + k_0^* k_L^* \Omega^2 \sin\Omega + k_0^* k_T^* \Omega^3 \cos\Omega - k_0^* \Omega^4 \sin\Omega \\ &+k_0^* k_L^* k_T^* \sin\Omega + k_L^* k_T^* \Omega^3 \cos\Omega - k_L^* \Omega^4 \sin\Omega = 0 \end{aligned} \tag{4.24}$$

The smallest positive root of this equation, say Ω_{cr}, yields the critical load

$$P_{cr}^* = \frac{\Omega_{cr}^2 EI}{L^2} \tag{4.25}$$

Buckling loads for beams having various special types of support conditions can be obtained through appropriate reduction of the general formulation (4.24). For the case of a finite torsional spring stiffness k_T^* and a finite vertical extensional spring stiffness k_L^*, but an infinite extensional spring stiffness k_0^*, the characteristic equation (4.24) reduces to

$$-k_L^* k_T^* \Omega \cos\Omega + k_L^* \Omega^2 \sin\Omega - \Omega^4 \sin\Omega + k_L^* k_T^* \sin\Omega = 0 \tag{4.26}$$

For the special case where one end of the beam is restrained by a torsional spring and a hinge while the other end is supported by a roller ($k_0 = k_L = \infty$). Equation (4.26) further reduces to

$$-k_T^* \Omega \cos\Omega + \Omega^2 \sin\Omega + k_T^* \sin\Omega = 0 \tag{4.27}$$

This case is represented by the curve labeled $k_L^* = \infty$ in Fig 6.1. In this case buckling load falls in the range of. $6.76 \le P_{cr}^* \le 13.153$

Next consider the case of one end rigidly clamped ($k_0^* = k_T^* = \infty$), and one end supported by a vertical spring. The characteristic equation (4.24) then reduces to

$$-k_L^*\Omega\cos\Omega+\Omega^3\cos\Omega+k_L^*\sin\Omega=0 \qquad (4.28)$$

The corresponding stability boundary is given by the curve labeled $k_T^*=\infty$ in Fig 6.2. In this case. $1.571 \le P_{cr}^* \le 13.153$

CHAPTER 5

MODAL ANALYSIS-Summary of steps

1. Main Menu> Preferences
2. (check) “Structural”
3. [OK]

5.1.2 Define Constant Material Properties

Here the material properties are specified as follows

Young’s modulus E =0 .724*10^{12} dyne/cm^2,

Poisons ratio =0.3,

Density, ρ = 2.77 gm/cm^3

Step followed are:

1. Select Main Menu> Preprocessor> Material Props> Material Models
2. Then double-click “Structural”, then “Linear”, then “Elastic”, then “Isotropic” and enter the values mentioned above and click [OK]
3. Now double-click on “Density”, enter density value, click [OK] and exit materials menu.

5.2. MODEL THE GEOMETRY

First key points are created, these key points are joined to form line segments and then using these lines areas are formed. The crack is modeled by creating two key points at the same coordinates and then using these key points two lines lying at the same location are created in transverse direction, these lines indicate crack

The steps followed are:

Main menu> Preprocessor> Modeling> Create> key points> In Active CS

Main menu> Preprocessor> Modeling> Create> Lines> line> Straight line

Main menu> Preprocessor> Modeling> Create> Areas> Arbitrary> By lines

5.3 GENARATE MESH

5.3.1 Element type

The recommended element type for a 2-D crack model is PLANE82 and SOLID95 for 3-D crack model. Combination14 is used for elastic support.

5.3.1(a). Plane82

PLANE82 element type is used for meshing the model. PLANE82 is a higher order version of the 2-D, four-node element (PLANE42). The 8-node element is defined by eight nodes having two degrees of freedom at each node: translations in the nodal x and y directions.

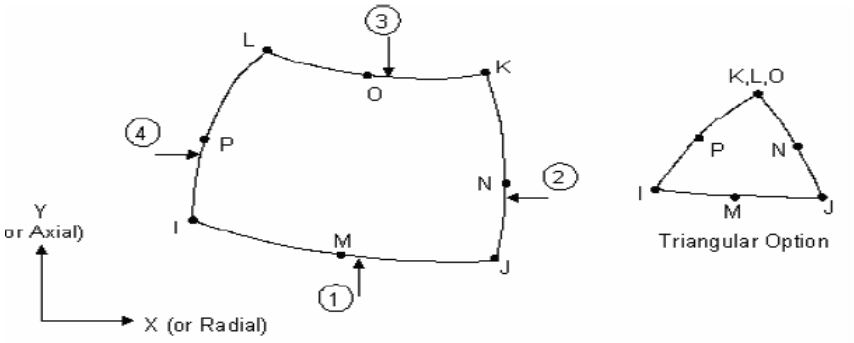

Figure 5.1 PLANE82 Element

The element may be used as a plane element or as an axis symmetric element. The element has plasticity, creep, swelling, stress stiffening, large deflection, Birth and death and large strain capabilities. A triangular-shaped element may be formed by defining the same node number for nodes K, L and O. A similar, but 6-node, triangular element is PLANE2.

Main menu> Preprocessor> Element type> Add/Edit/Delete> Add> Solid> PLANE82

5.3.1.1 Modeling crack region

The most important region in a crack model is the region around the edge of the crack. The edge of the crack is referred as a *crack tip* in a 2-D model and *crack front* in a 3-D model. To pick up the singularity in the strain, the crack faces should be coincident, and the elements around the crack tip (or crack front) should be quadratic, with the

5. MODAL ANALYSIS -- SUMMARY OF STEPS

Following steps show the guidelines for carrying out Modal analysis. Details step by step explanation is presented in further sections.

5.1 Define Materials

1. Set preferences. (Structural)
2. Define constant material properties.

5.2 Model the Geometry

3. Follow bottom up modeling and create the geometry

5.3 Generate Mesh

4. Define element type.
5. Mesh the area.

5.4 Apply Boundary Conditions

8. Apply constraints to the model.

5.5 Obtain Solution

9. Specify analysis types and options.
10. Solve.

5.1 DEFINE MATERIALS

5.1.1 Set Preferences

Purpose of setting preferences is to filter quantities that pertain to this discipline only. On clicking preference option, many disciplines are listed like structural, thermal, electromagnetic, fluid etc. here structural option is checked out and so only quantities related to structural analysis will be highlighted. Step followed are:

midside nodes placed at the quarter points. Such elements are called *singular elements* shown in figure 5.2. Figure 5.2 shows singular element for 2_D crack modeling. The element is plane2.It is defined by 6 nodes with 2 degrees of freedom at each node, translation along X and Y directions.

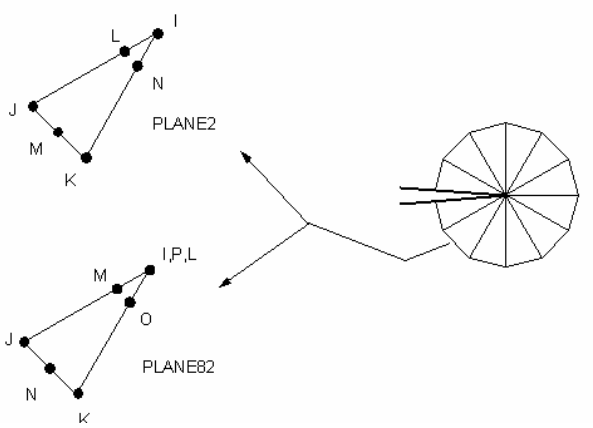

Figure 5.2 plane2 element

The first row of elements around the crack tip should be singular. By creating a concentrate key point is at the crack tip, singular elements are automatically generated around the specified key point, i.e. the crack tip. The following steps are followed.

Main Menu> Preprocessor> Meshing> Size Controls> Concentrat KPs> Create.

For good results, the first row of elements around the crack tip should have a radius of approximately *a*/8 or smaller, where '*a*' is the crack length. In the circumferential direction, roughly one element every 30° or 40° is recommended.

5.3.1(b) Combination14

COMBIN14 is used for elastic supports at the two ends of the model. It has longitudinal or torsional capability in 1-D, 2-D, or 3-D applications. The longitudinal spring-damper option is a uniaxial tension-compression element with up to three degrees of freedom at each node: translations in the nodal x, y, and z directions. No bending or torsion is considered. The torsional spring-damper option is a purely rotational element with three degrees of freedom at each node: rotations about the nodal x, y, and z axes. No bending or axial loads are considered.

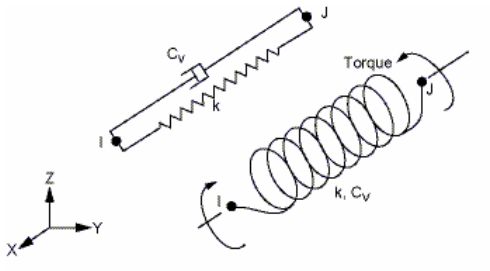

Fig.5.3. Combin14 element

The spring-damper element has no mass. Masses can be added by using the appropriate mass element. The spring or the damping capability may be removed from the element. The damping capability is not used for static or undamped modal analyses.

5.3.2 Meshing

The area is free meshed, using quadrilateral Plane82 elements as shown in figure 5.3.3(b). Before meshing it's important to define the crack tip and then create a very fine mesh surrounding the crack region. The elements around the crack tip are skewed, i.e. the mid side nodes are moved nearer to the crack tip as shown in the figure 5.3.3(b) below. The area away from the crack is meshed coarsely.

Main menu> Preprocessor> Meshing> Mesh tool> Set> lines give desired divisions
Main menu> Preprocessor> Meshing>Size control> concentrate KPs> create
Main menu> Preprocessor> Meshing> Mesh tool> Mesh>areas

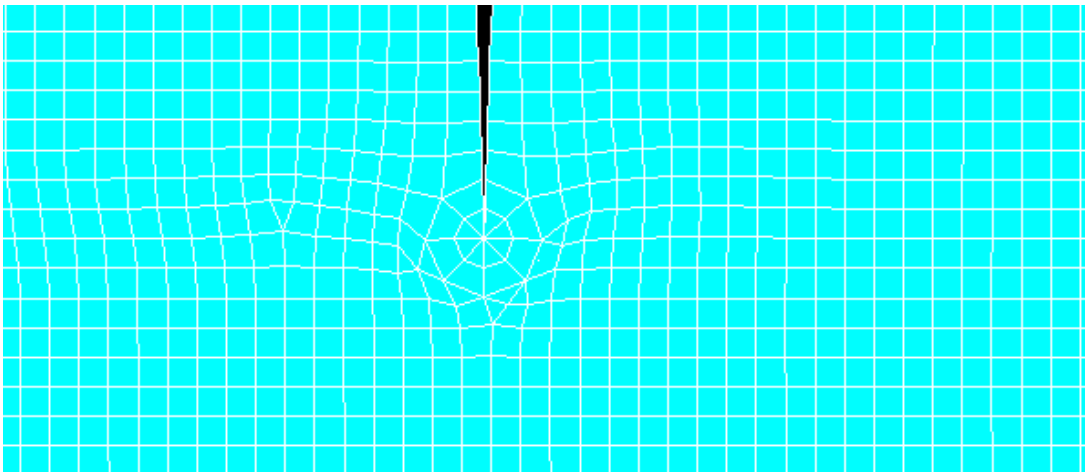

Fig 5.4 Meshing of crack region in ANSYS

5.4. Applying Boundary Conditions and Solving

The nodes of linear spring support and torsional spring support at one end (starting) of the cantilever beam are restricted in all degree of freedom for and nodes of the beam at that end also restricted along X direction . The nodes of linear spring at the other of the beam are restricted in Y direction. First static analysis is carried out and then the analysis type is changed from static to modal analysis. In modal analysis, the number of modes to be extracted is specified. The numbers of modes extracted are 3 and then they are expanded to view the results. No external load is given as this is free vibration analysis. Then this model is solved for the results.

Main menu> Solution>Analysis type> New analysis>Modal
Main menu> Solution>Define loads> Apply> Structural> Displacements> on nodes

5.5 Viewing results and saving

To view the results first mode results should be read. We can view the different natural frequencies and mode shapes. The frequency for different modes shapes are listed as result summary. After completing all these file has to be saved by a file name for future viewing and modifications.

The above steps are repeated for different conditions like single crack of 0.06mm, 1mm, 2mm and3mm depth and with no crack.

CHAPTER 6

RESULTS AND DISCUSSIONS

6. RESULTS&DISCUSSIONS

6.1 NUMERICAL RESULTS

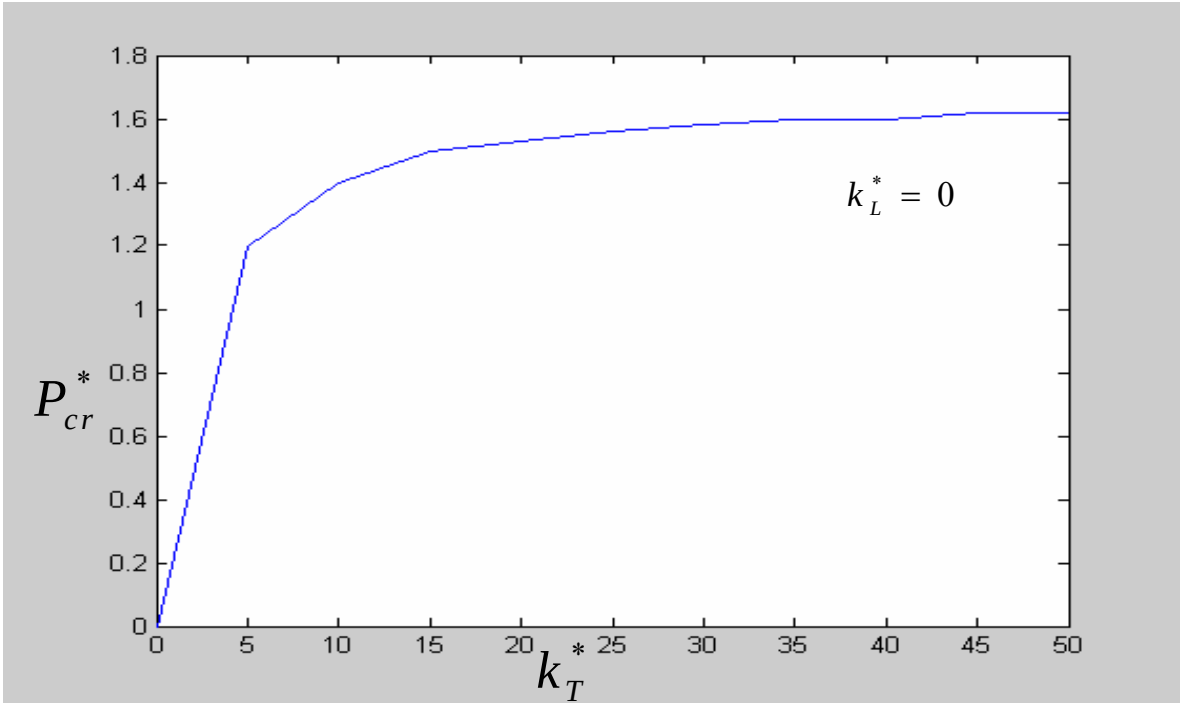

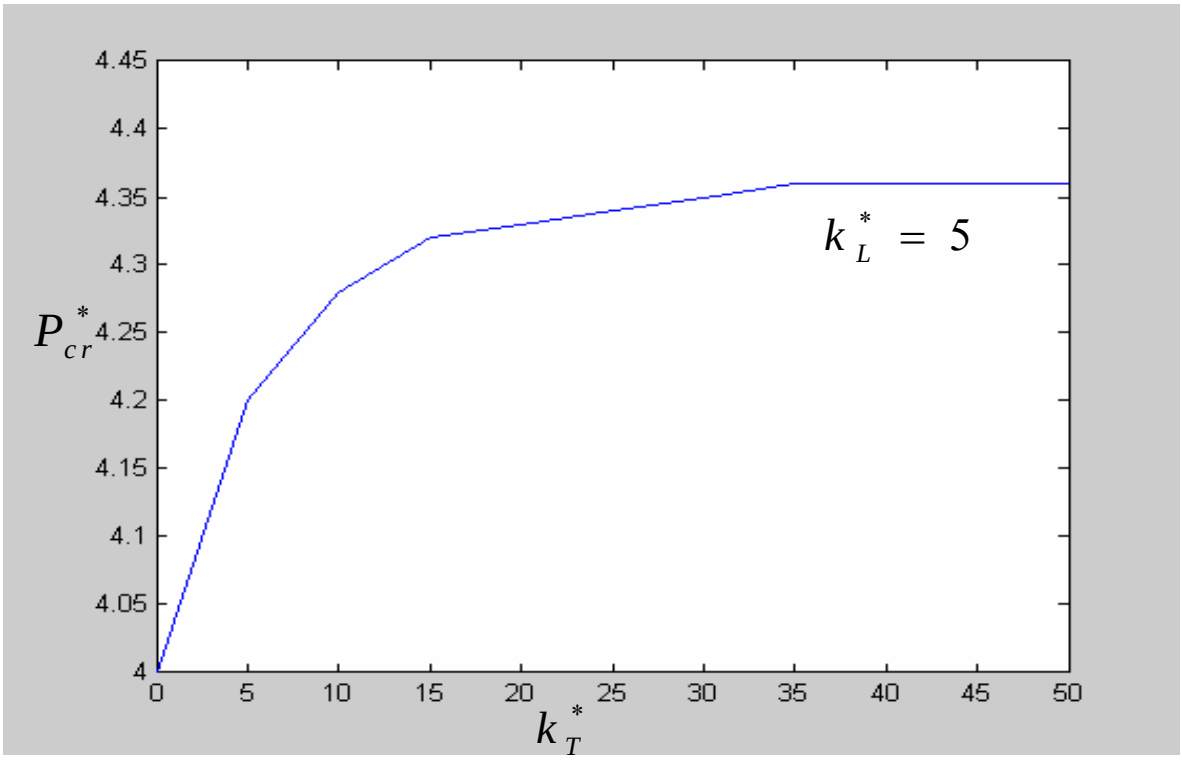

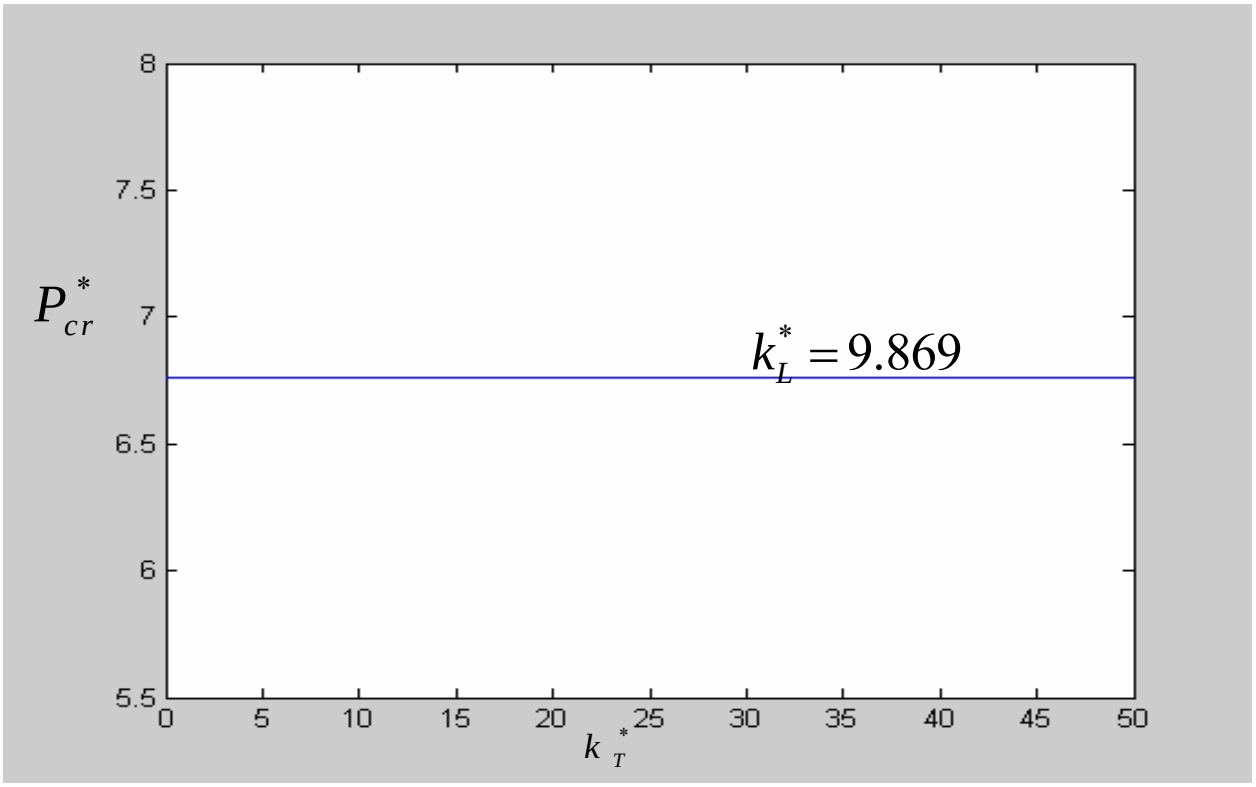
8
7.5
7
6.5
6
5.5
0
5
10
15
20
25
30
35
40
45
50
P^*_{cr}
$k^*_L = 9.869$
k^*_T

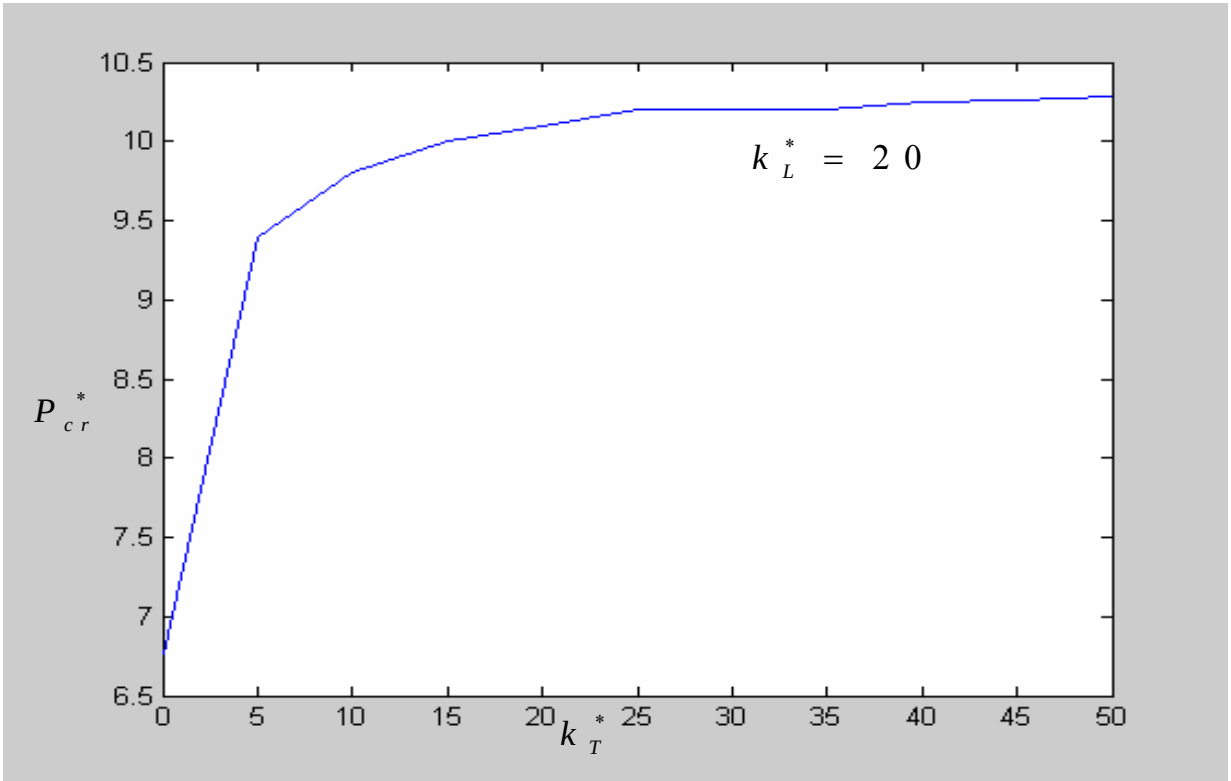
10.5
10
9.5
9
8.5
8
7.5
7
6.5
0
5
10
15
20
25
30
35
40
45
50
P^*_{cr}
$k^*_L = 20$
k^*_T

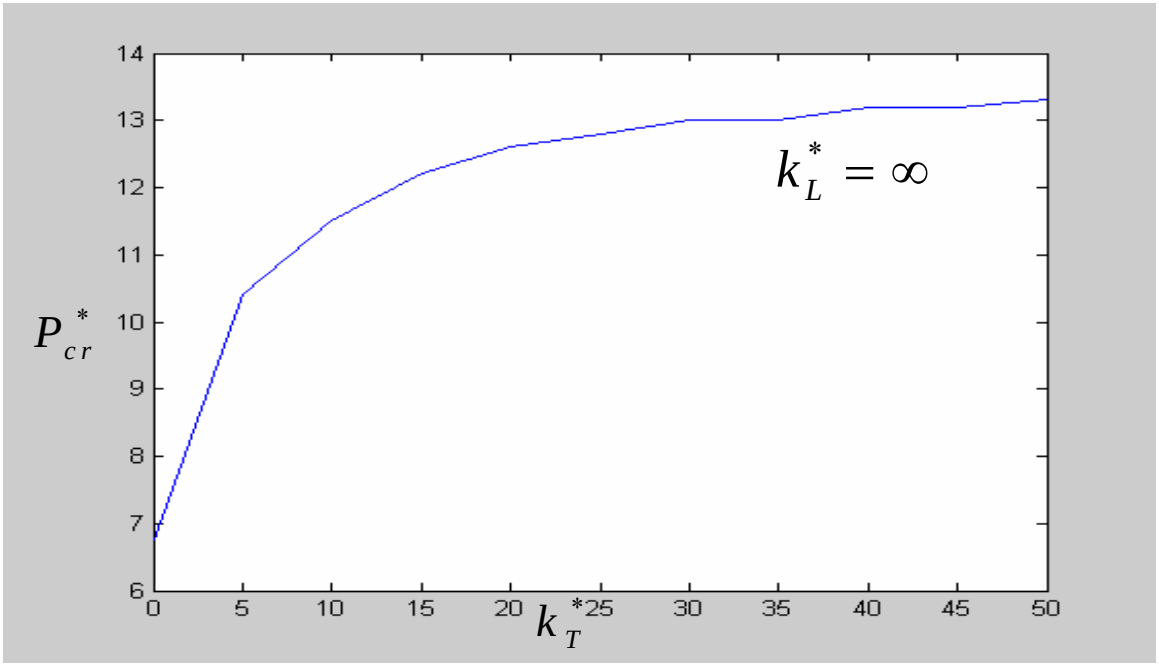

Fig 6.1. Stability boundaries for the elastically supported beam. $K_0^* = \infty$

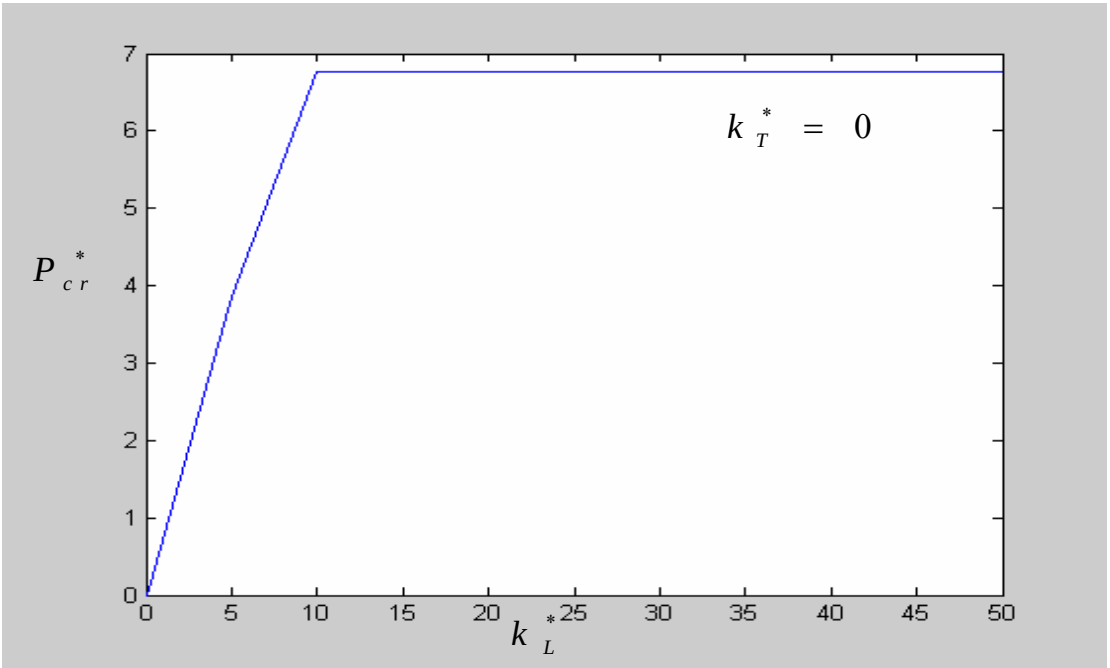

.

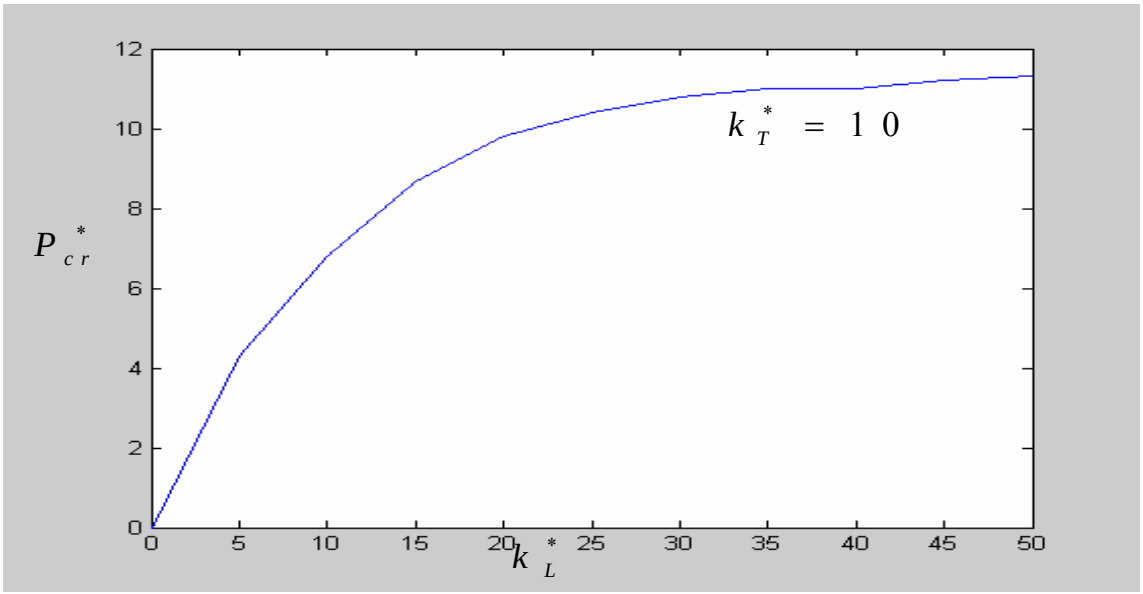
$k_T^* = 10$
P_{cr}^*
k_L^*
0
2
4
6
8
10
12
0
5
10
15
20
25
30
35
40
45
50

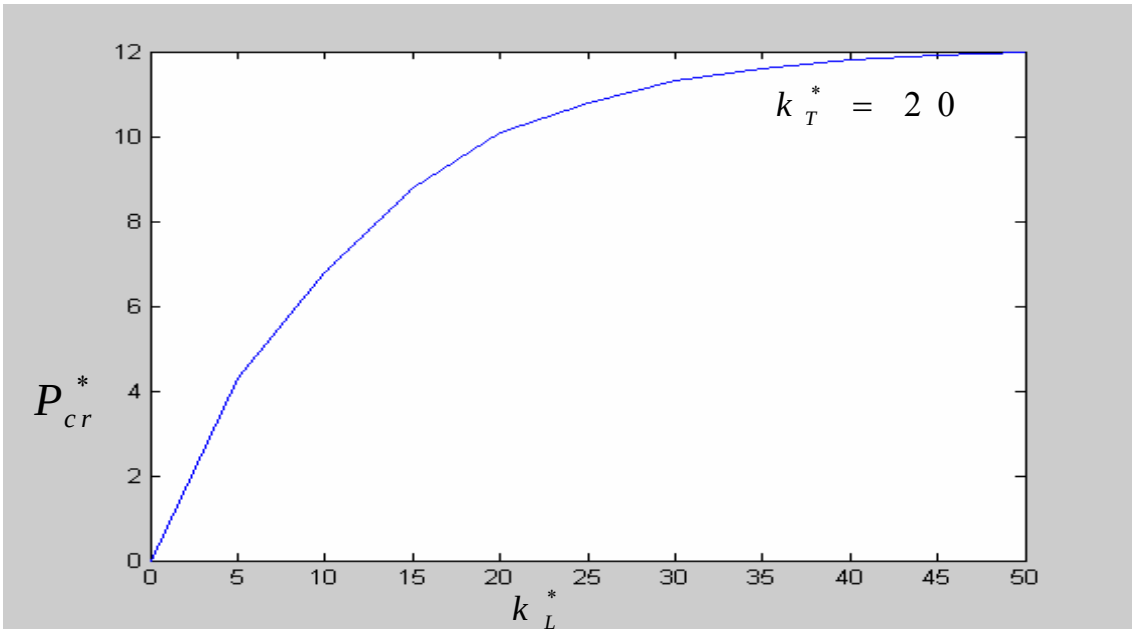
$k_T^* = 20$
P_{cr}^*
k_L^*
0
2
4
6
8
10
12
0
5
10
15
20
25
30
35
40
45
50

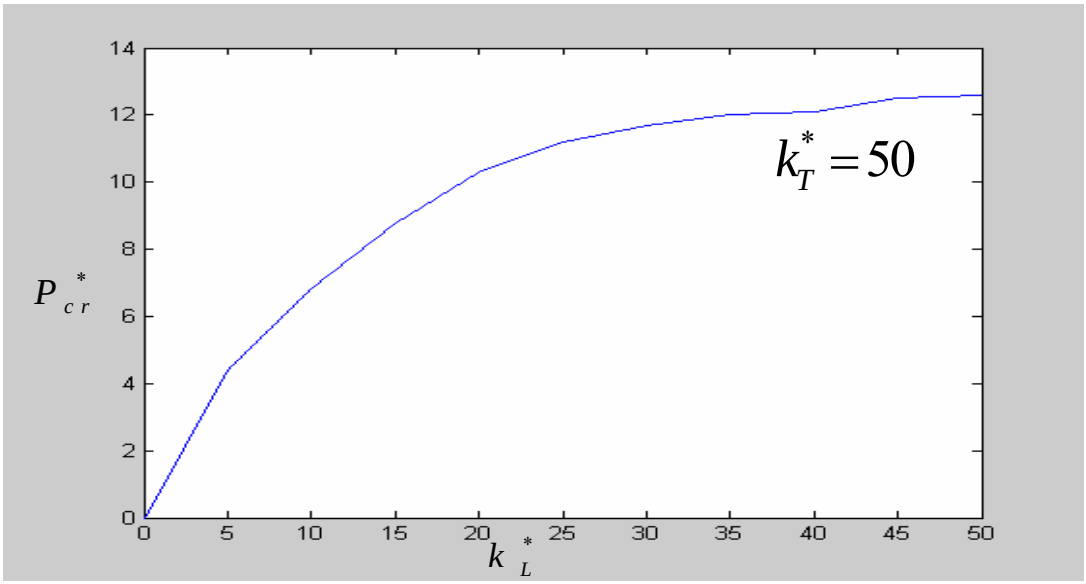

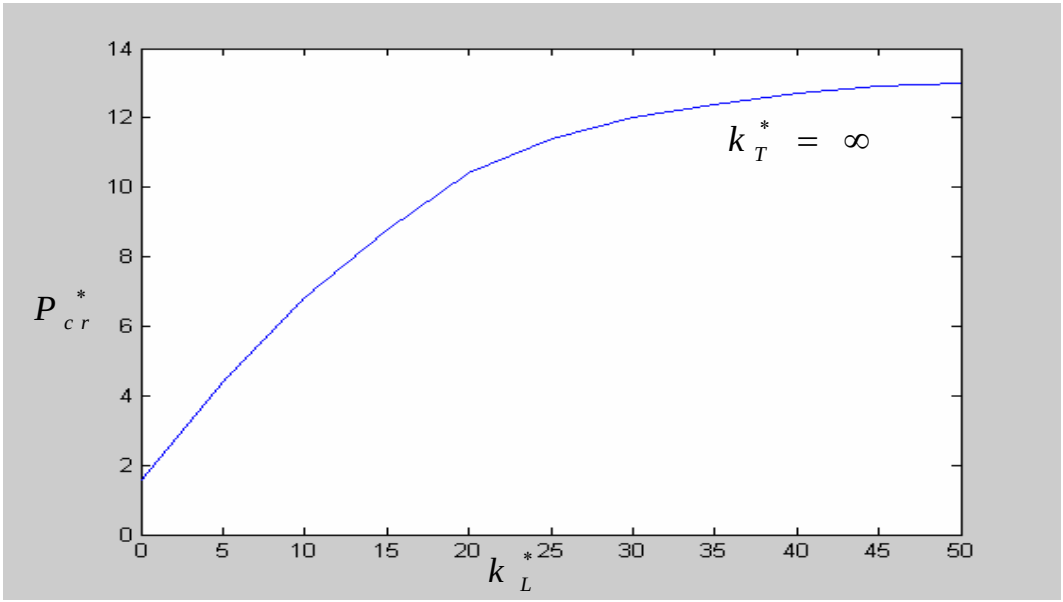

Fig 6.2 Stability boundaries for the elastically supported beam, $k_0^* = \infty$.

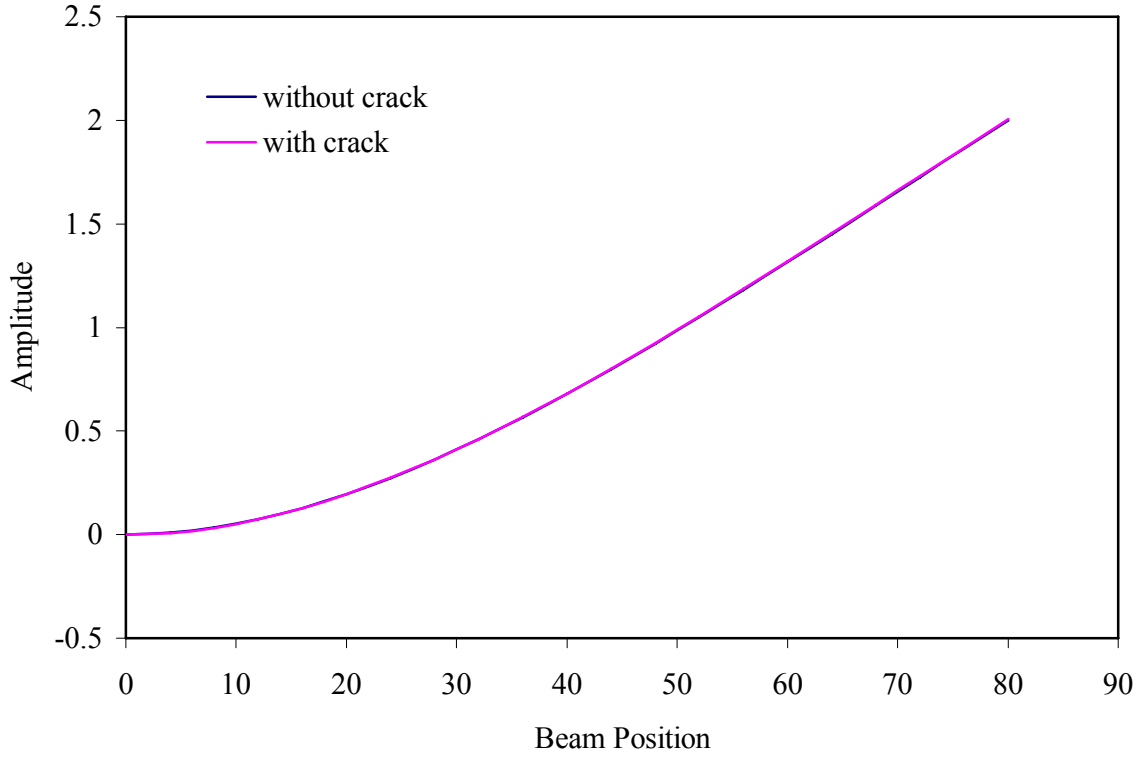

Fig.6.3 First mode of transverse vibration ,a/w=0.01,L1/L=0.125

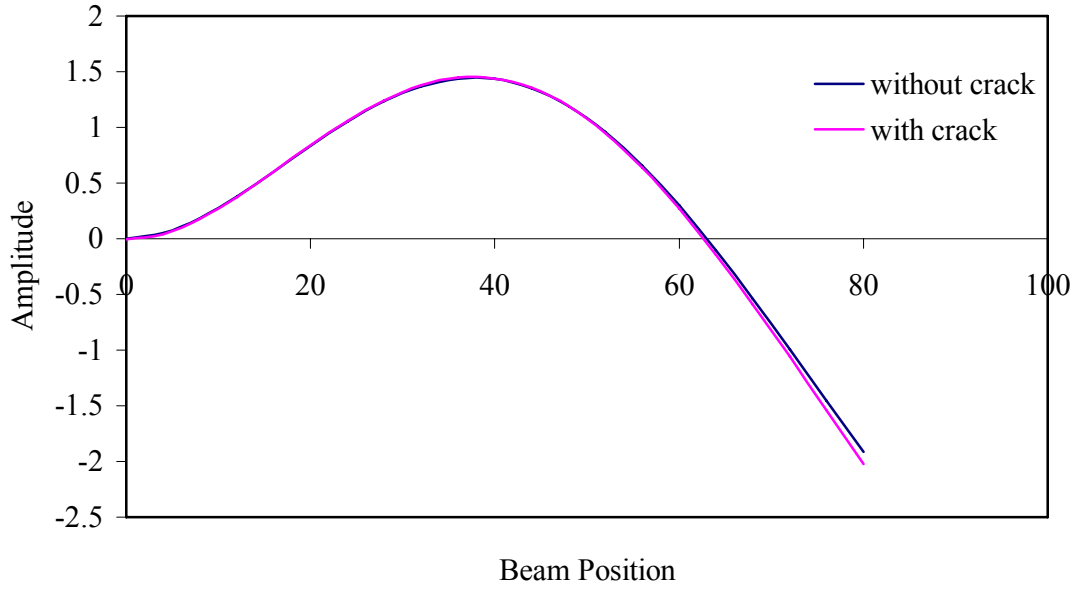

Fig 6.4 Second mode of transverse vibration ,a/w=0.01,L1/L=0.125

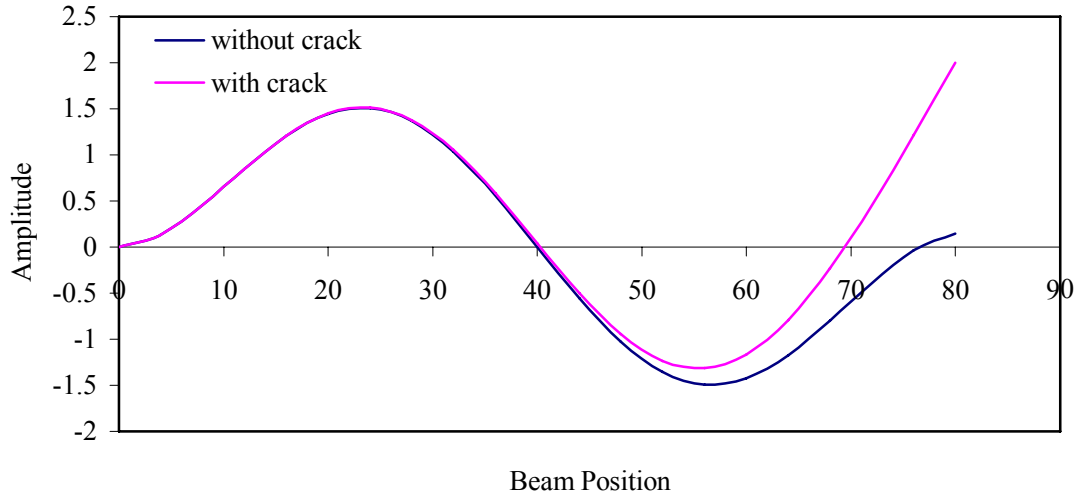

Fig 6.5.Third mode of tranverse vibration,a/w=0.01,L1/L=0.01

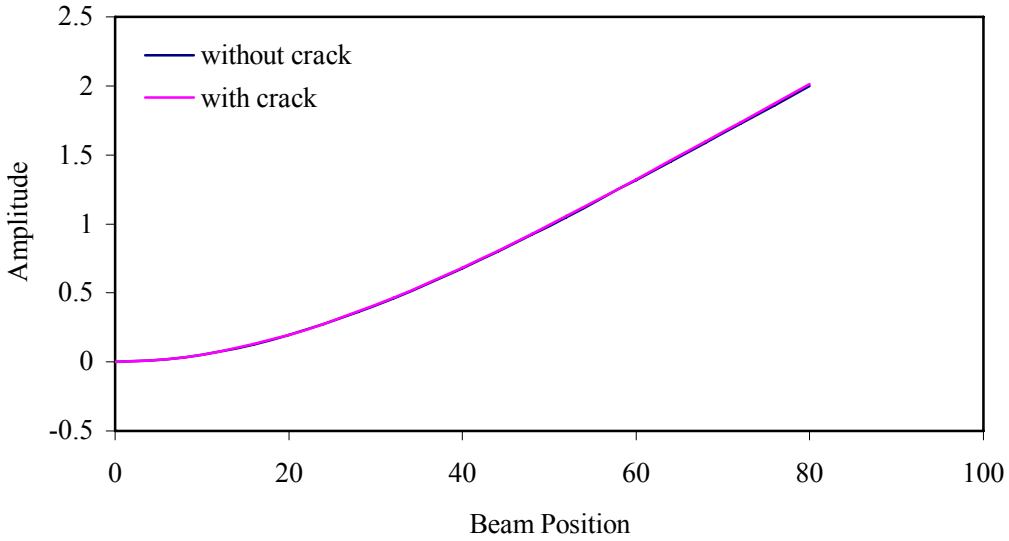

Fig 6.6 First mode of transverse vibration,a/w=0.1667,L1/L=0.125

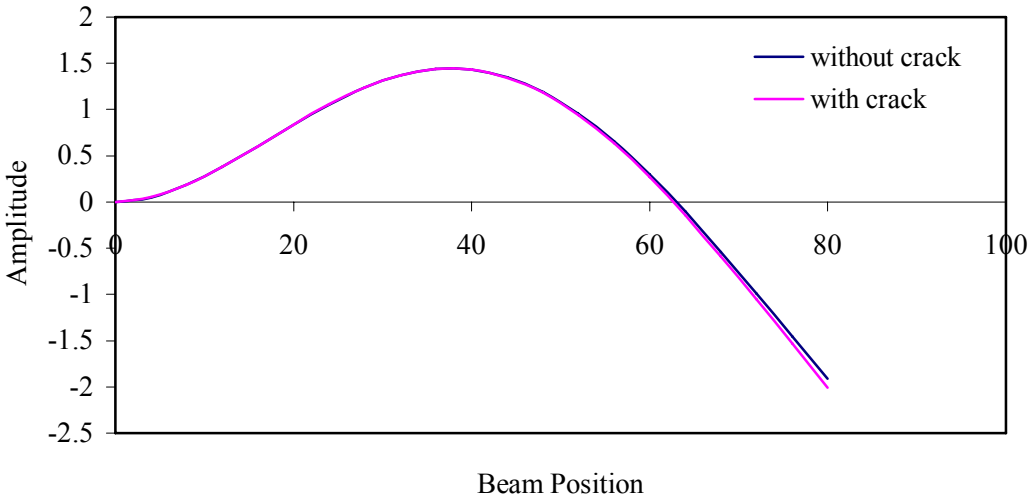

Fig 6.7.Second mode of transverse vibration,a/w=0.1667,L1/L=0.125

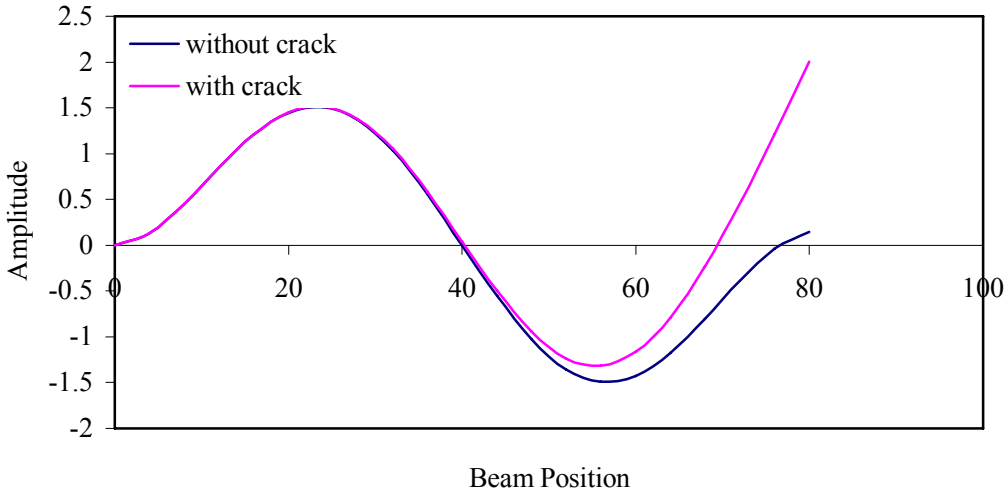

Fig 6.8.Third mode of transverse vibration,a/w=0.1667,L1/l=0.125

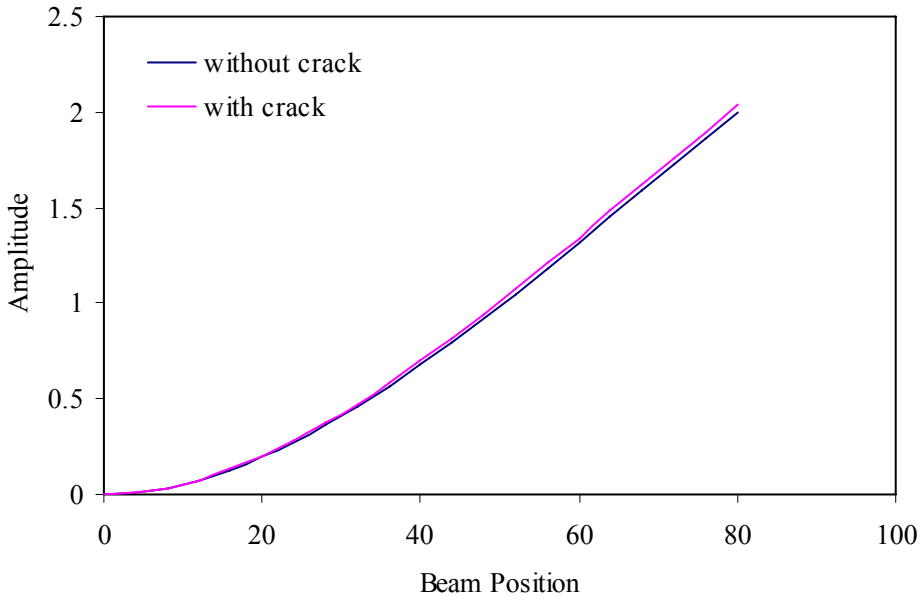

Fig 6.9 first mode of transverse vibration,a/w=0.334,L1/l=0.125

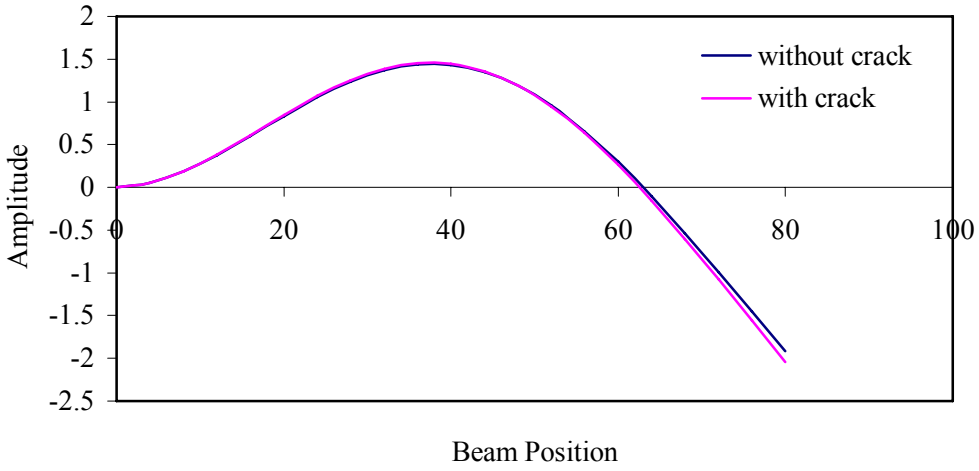

Fig 6.10 Second mode of transverse vibration ,a/w=0.334

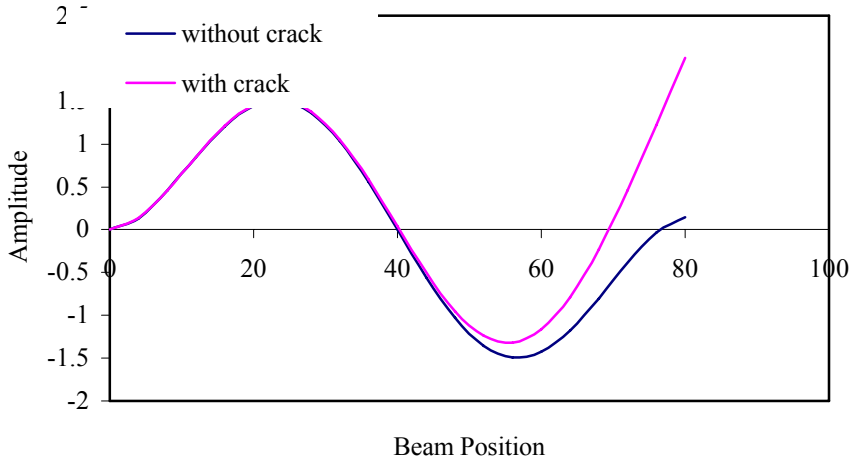

Fig.6.11 Third mode of transverse vibration,a/w=0.334,L1/L=0.125

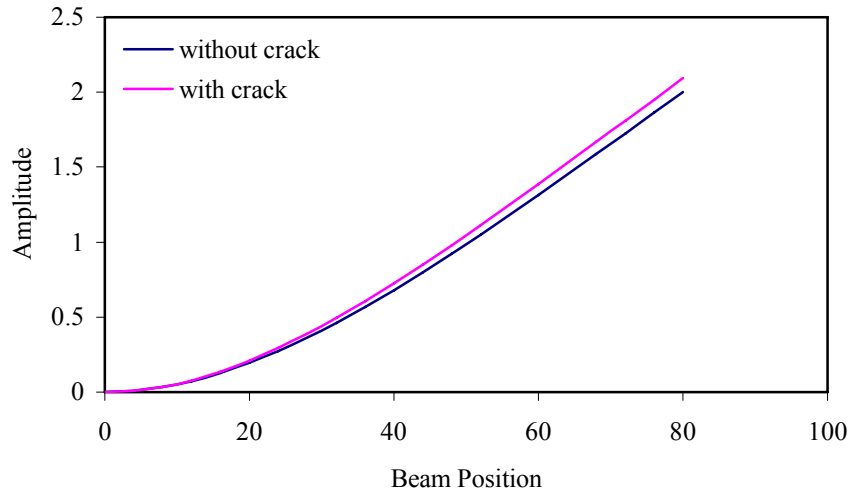

Fig. 6.12 First mode of transverse vibration,a/w=0.5,L1/L=0.125

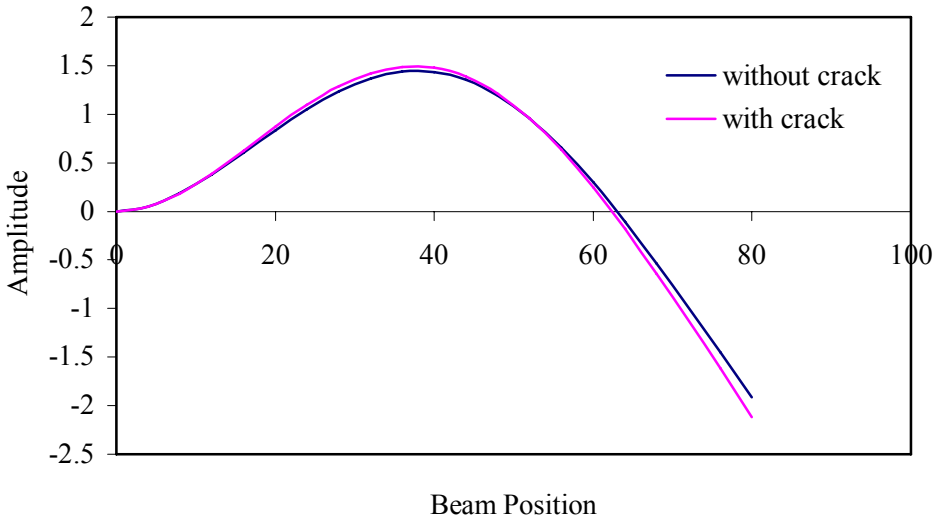

Fig 6.13. Second mode of transverse vibration.a/w=0.5,L1/L=0.125.

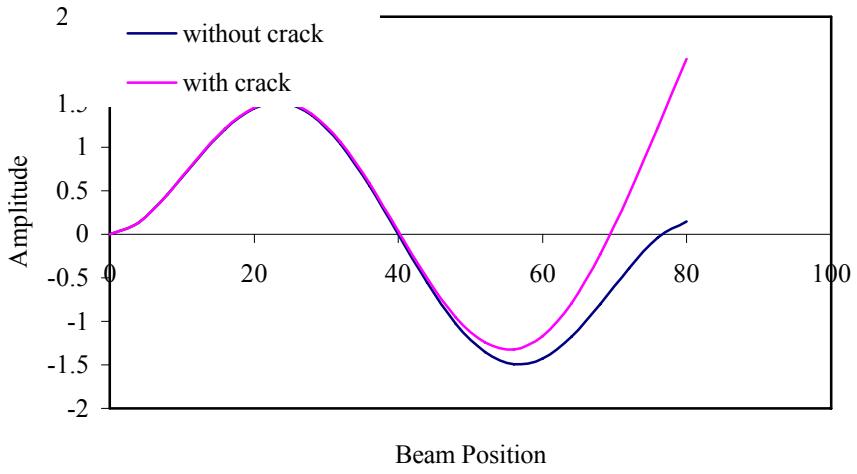

Fig 6.14 Third mode of transverse vibration,a/w=0.5,L1/l=0.125

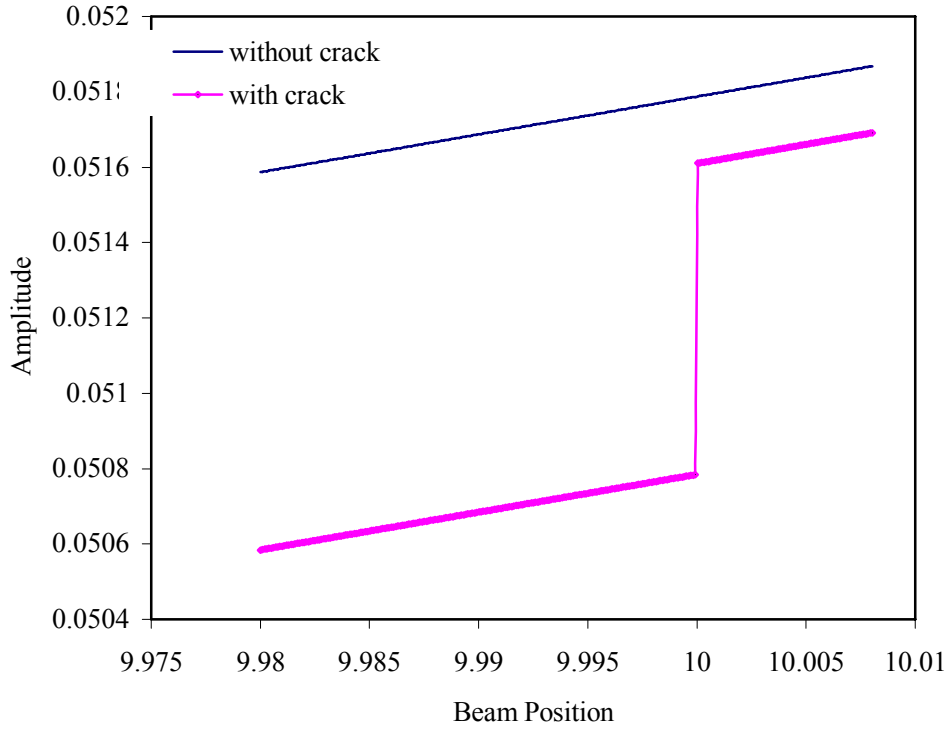

Fig 6.15 First mode of transverse vibration,a/w= 0.01,L1/L=0.125

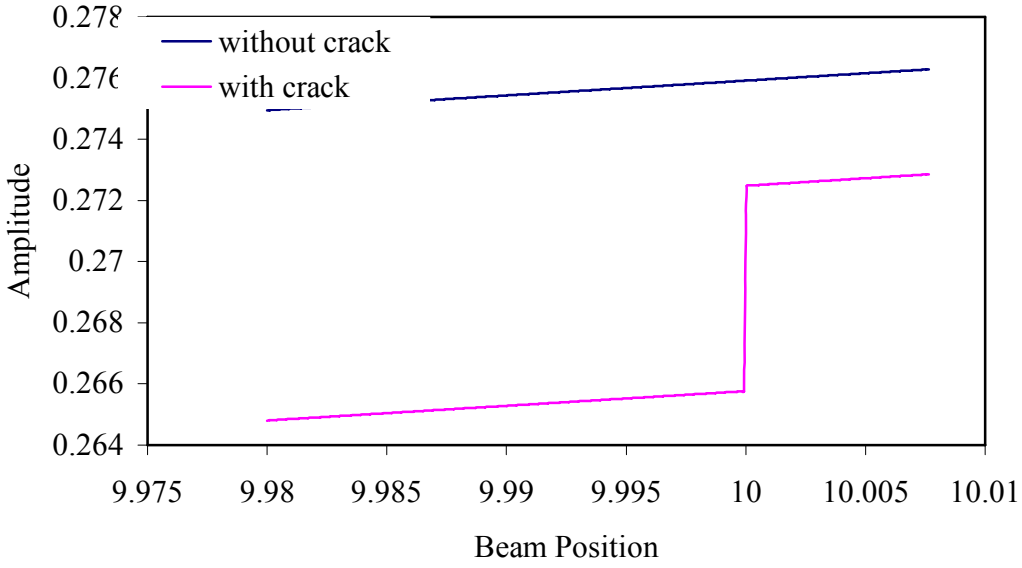

Fig 6.16 Second mode of transverse vibration,a/w= 0.01,L1/L=0.125

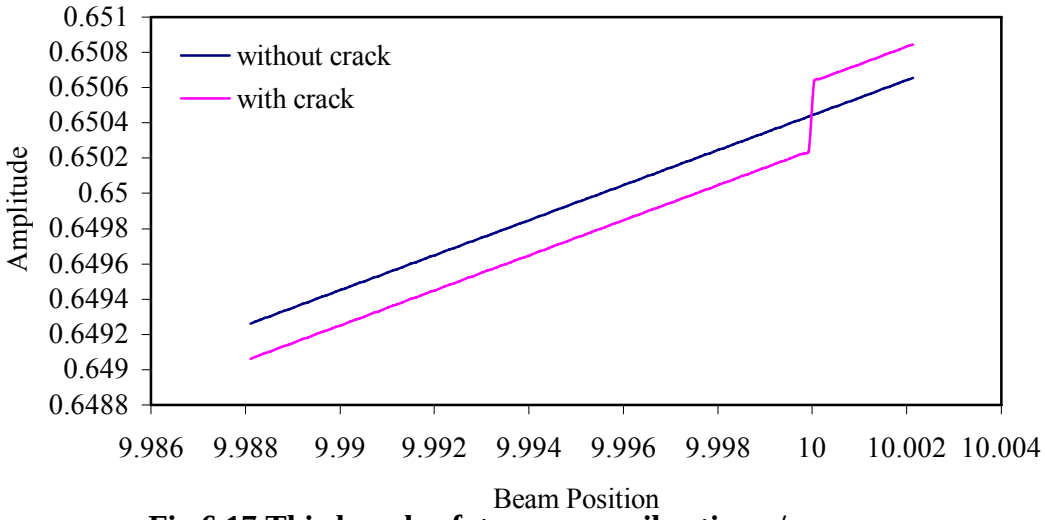

Fig 6.17 Third mode of transverse vibration,a/w= 0.01,L1/L=0.125

Relative crack depth	Frequency of First eigen value	Frequency found out in ANSYS
0.01	48.2	48.22
0.1667	48.0988	48.099
0.334	47.7	47.77
0.5	46.84	46.9
0.6	45.709	45.715
0.7	43.48941	43.4895
0.8	38.5589	38.5596
0.9	26.26	26.265
0.99	3.175	3.1772

Table 6.1 Variation of first eighen value frequency with respect to relative crack depth.

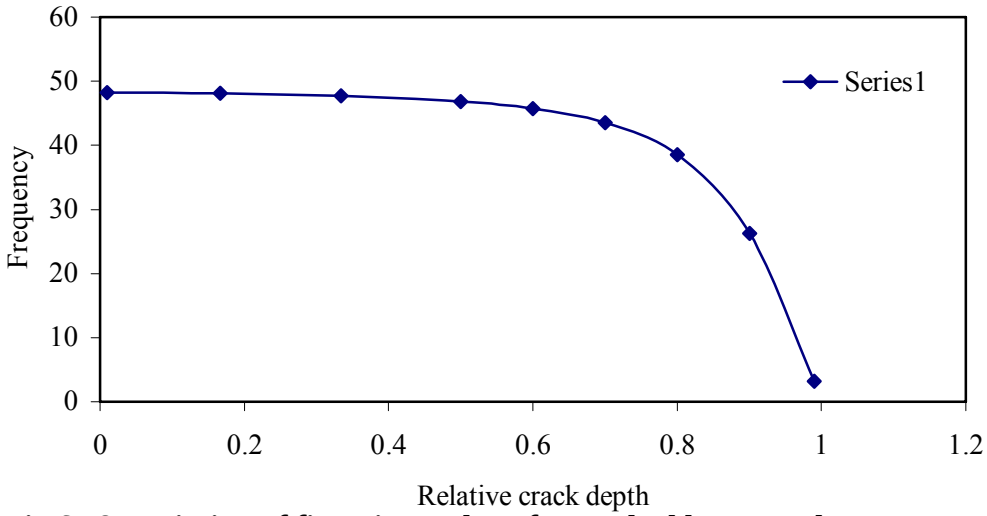

Fig 6.18 Variation of first eigenvalue of a cracked beam vs.the relative crack depth

Relative crack depth	Frequency of second eigen value	Frequency found out in ANSYS
0.01	96.39	96.28
0.1667	96.0309	96.0314
0.334	95.066	95.07
0.5	93.18	93.18
0.6	90.818	90.822
0.7	86.27882	86.2789
0.8	76.3178	76.318
0.9	51.62	51.55
0.99	5.36	5.42

Table 6.2. Variation of second eighenvalue of a cracked beam vs.the relative crack depth.

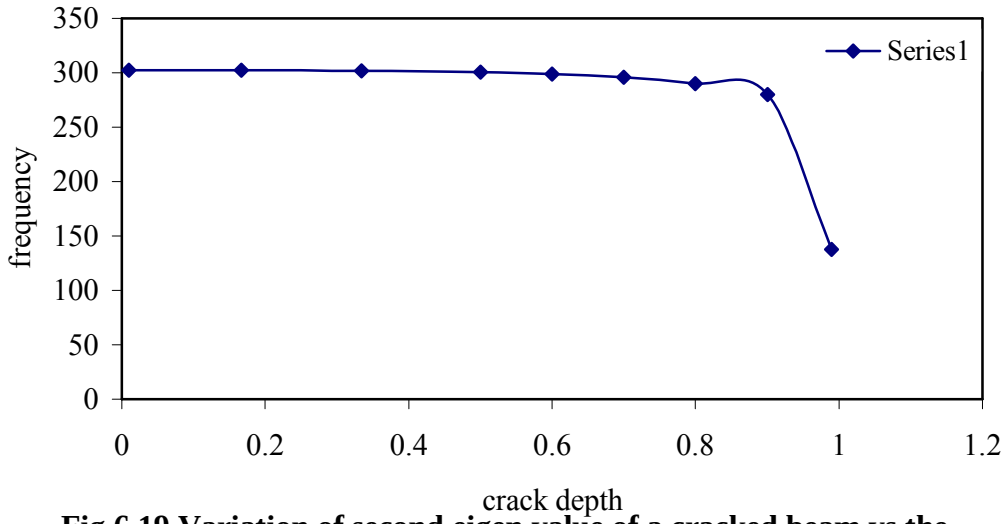

Fig 6.19.Variation of second eigen value of a cracked beam vs.the crack depth

Relative crack depth	Frequency of third eigen value	Frequency found out in ANSYS
0.01	144.58	144.62
0.1667	143.96	143.97
0.334	142.43	142.45
0.5	139.52	139.57
0.6	135.93	135.97
0.7	129.07	129.09
0.8	114.08	114.095
0.9	76.98	76.88
0.99	7.54	7.59

Table 6.3 Variation of third eighen value of a cracked beam vs. the crack depth

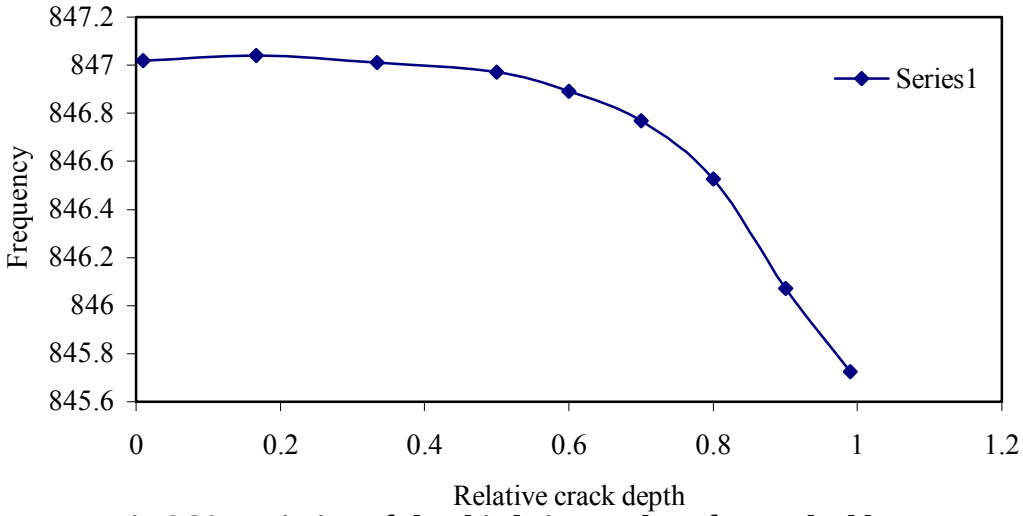

Fig 6.20.Variation of the third eigen value of a cracked beam vs. relative crack depth

6.2 SIMULATION RESULTS

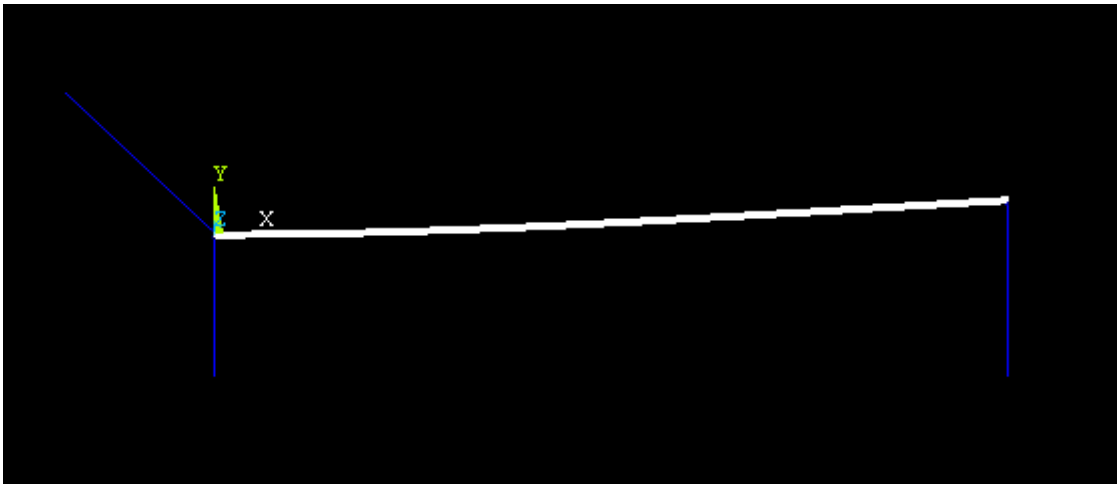

Figure 6.21. First mode of tranverse vibration for uncracked beam

Figure 6.22. Second mode of transverse vibration for uncracked beam

Figure 6.23 Third mode of transverse vibration for uncracked beam

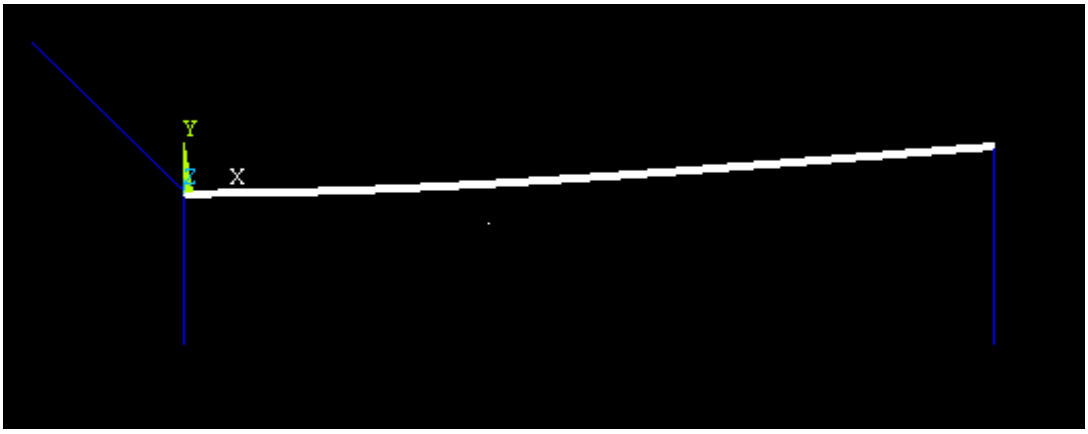

Figure 6.24. First mode of transverse vibration, a/w=0.01,L_1/L=0.125

Figure 6.25. Second mode of transverse vibration,a/w-0.01,L_1/L=0.125

Figure 6.26.Third mode of transverse vibration, a/w=0.01,L_1/L=0.125

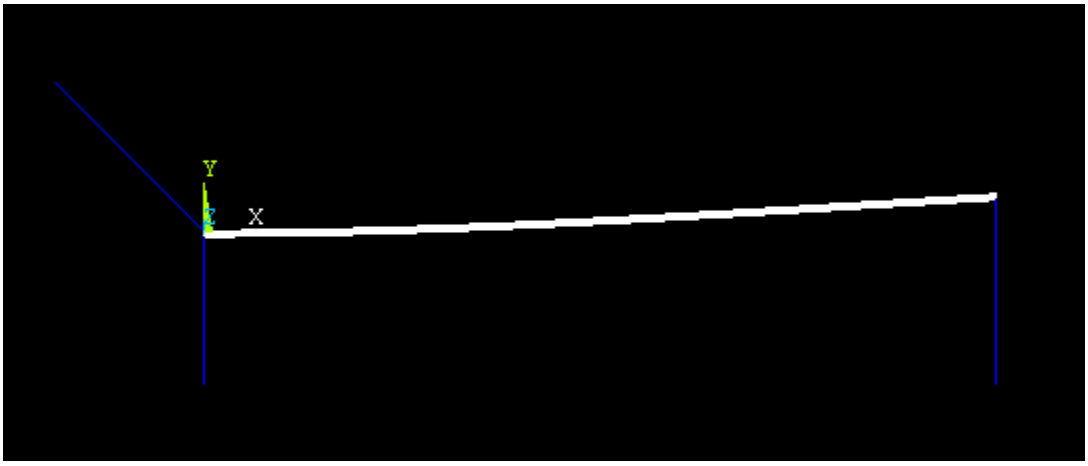

Figure 6.27.First mode of transverse vibration,a/w=0.1667, L_1/L=0.125

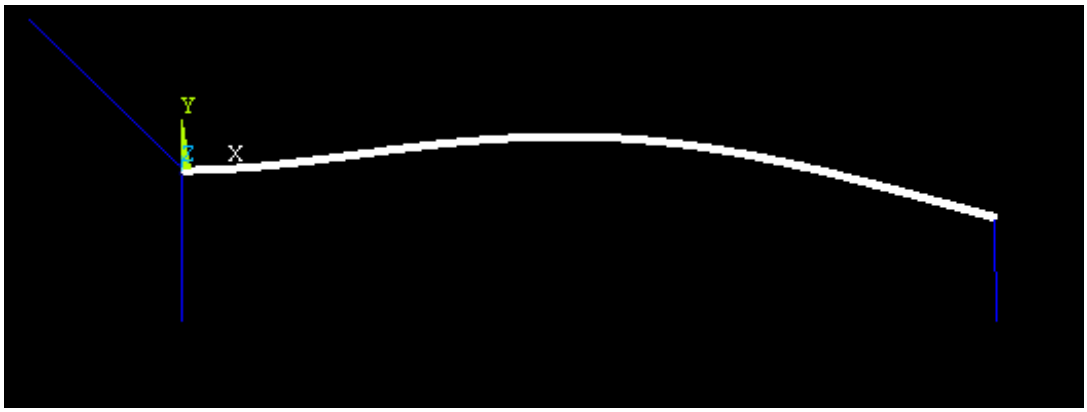

Figure 6.28. Second mode of transverse vibration, a/w=0.1667,L_1/L=0.125

Figure 6.29. Third mode of transverse vibration, a/w=0.1667,L_1/L=0.125

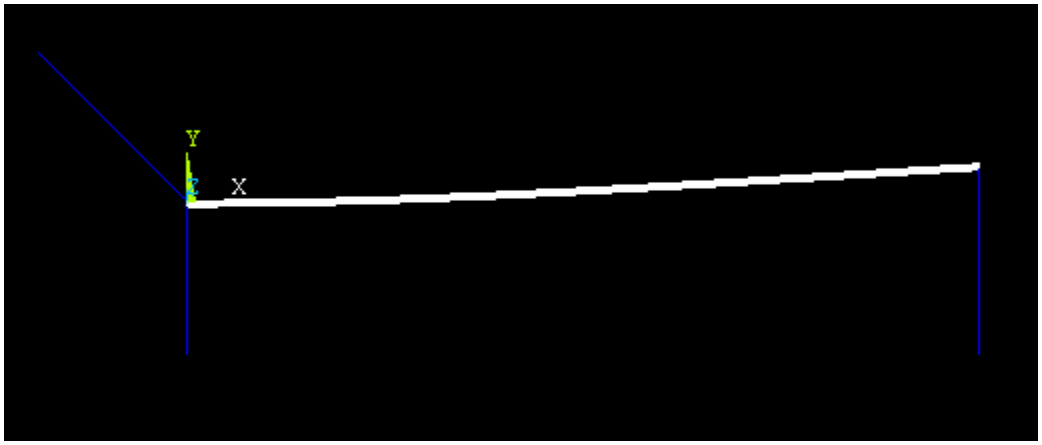

Figure 6.30. First mode of transverse vibration,a/w=0.334,L_1/L=0.125

Figure 6.31. Second mode of transverse vibration, a/w=0.334,L_1/L=0.125

Figure 6.32. Third mode of transverse vibration, a/w=0.334,L_1/L=0.125

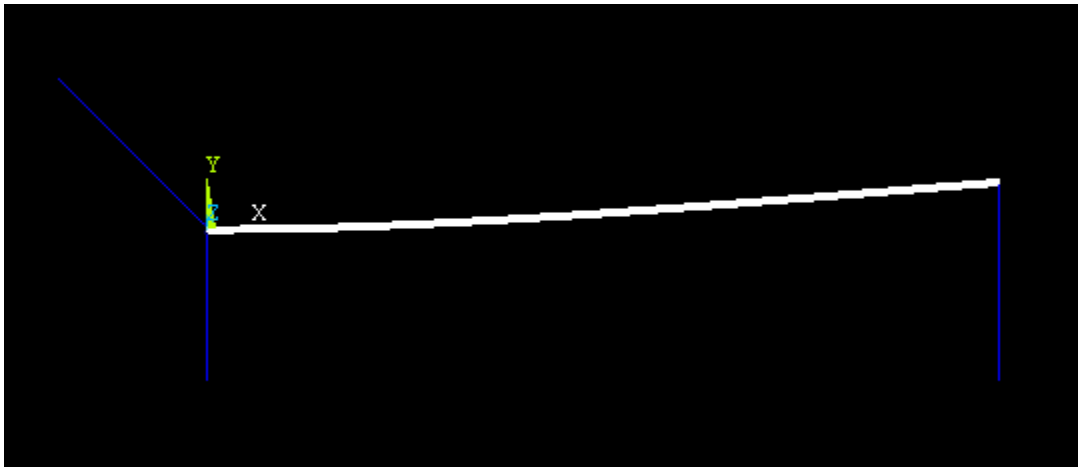

Figure 6.33.First mode of transverse vibration, a/w=0.5,L_1/L=0.125

Figure 6.34.Second mode of transverse vibration, a/w=0.5,L_1/L=0.125

Figure 6.35.Third mode of transverse vibration, a/w=0.5,L_1/L=0.125

6.3 DISCUSSIONS

An aluminium beam with elastic springs ($k_0 = 10^{44}, k_L = 0, k_T = 10^{44}$) with a uniform cross-section area of 80 cm,breadth 5 cm, depth 6 mm, modulus of elasticity E=0.724×10^{12} dynes/cm^2, Poisson's ratio (υ)=0.3, and density (ρ)=2.77 gm/cm^3 is considered for the numerical analysis. The crack is situated at one position (L_1/L=10/8=0.125). The crack depths are chosen such that a/w=0.01,0.1667,0.334 and 0.5. The first, second, and third natural frequencies corresponding to various crack conditions are calculated. The fundamental mode shapes for trasverse vibration of cracked and uncracked beams are plotted and compared. The magnified view of the mode shapes is also plotted for the elastic beams in the vicinity of the crack in order to observe the change in the mode shape. The numerical results are shown in Figs.6.3-6.20.The simulation results obtained by ANSYS software are shown in Figs.6.21-6.35. The critical load found out for two different end conditions are shown in Figs.6.1 and 6.2.

The results obtained from the numerical analysis are presented in graphical forms. In Fig 6.13.It is evident that there is an appreciate variation between the natural frequency of cracked and uncracked cantilever beams. With the increase in mode of vibration this difference increases. The transverse vibration first, second and third mode shapes for single crack aluminium beam are shown in Figs.(6.3)-(6.5).In these figures, the relative crack depth considered is 0.01.In Figs. 6.6-6.8 the relative crack depth considered is 0.1667 . In Figs. 6.9-6.11 the relative crack depths are considered as 0.334. In Figs. 6.12-6.14 the relative crack depth considered as 0.5.and in figures (6.3)–(6.14) the relative crack position is fixed at 0.125.

For moderate cracks (a/w=0.1667) appreciable changes in mode shapes are noticed and for deep cracks (a/w=0.5) the change in mode shapes are quite substantial. Further more, the numerical results indicate that the deviation between the fundamental mode shapes of the cracked and uncracked beam is always sharply changes at the crack location. Such behaviours are noticed in the magnified views of the mode shapes (Figs. 6.15-6.17. The changes of natural frequencies with respect to crack depths are shown in

Figs.6.18-6.20. Measurable changes in natural frequencies can be observed for relatively deep cracks.

For minute crack (a/w=0.01) the magnified views of transverse mode shapes at the crack locations are depicted in Figs.6.15-6.17. From these figures it is observed that the mode shapes change sharply at the crack locations.

Figs. 6.1 and 6.2 show the stability boundaries for elastically supported columns for two conditions. One is at one end of the column restrained by a torsional spring and a hinge while the other end is supported by roller. Secondly, one end rigidly clamped and the other end is supported by a vertical spring. For these two cases, the critical loads are found out. The curves in these figures represent stability boundaries, i.e. points below these curves correspond to values of load P^* and stiffnesses k_T^*, k_L^* for which the beam is remains in a stable unbuckled state.

CHAPTER 7

CONCLUSIONS AND SCOPE FOR FURTHER WORK

7. CONCLUSION& SCOPE FOR FURTHER WORK

The numerical results are shown in fig 6.3-6.20 and the simulation analysis results are shown in fig 6.21-6.35.it is observed that the natural frequency of beam for a single crack decreases as compared to the uncracked cantilever beam condition. The frequency of the cracked cantilever beam decreases with increase in the crack depth for the all modes of vibration.

For minute crack depth there is minor change in mode shapes between the cracked and uncracked beam. For moderate crack depth (a = 3mm) the change in mode shapes are quite substantial. For deep crack (a ≥ 5mm) the change in mode shapes can be easily distinguished.

In the case of one end of the beam restrained by a torsional spring and a hinge while the other end is supported by roller ($k_0^* = k_L^* = \infty$), the critical load found out in the range of $6.76 \leq P_{cr}^* \leq 13.153$ as shown in fig 6.1

In the case of one end rigidly clamped ($k_0^* = k_T^* = \infty$), and one end supported by a vertical spring (Fig 6.2), the critical load found out in the range of $1.571 \leq P_{cr}^* \leq 13.153$

FURTHER WORK

- The cracked cantilever can be analyzed under the influence of external forces.
- The dynamic response of the cracked beams can be analyzed for different crack orientations
- Stability study of the cracked beams can be done.

CHAPTER 8

REFERENCES

8. REFERENCES

1. Irwin, G.R., analysis of stresses and strains near the end of a crack traversing a plate, Journal of Applied Mechanics, 1957, 24,361-364.
2. Irwin, G.R., Relation of stresses near a crack to the crack extension force. 9th Congress Applied Mechanics, Brussels, 1957.
3. Krawczuk, M. and Ostachowicz. W.M., Transverse natural vibrations of a cracked beam loaded with a constant axial force. Journal of Vibration and acoustics, Trans. ASME, 1993,115, pp.428-524.
4. Ostachowicz. W.M. and Krawczuk, M., Analysis of the effect of cracks on the natural frequencies of a cantilever beam. Journal of Sound and vibrations.1991, 150, pp.191-201.
5. Ostachowicz. W. M. and krawczuck, M., Coupled torsional and bending vibrations of a rotor with an open crack. Archive of Applied Mechanics, Vol. 62, 1992, pp.191-201.
6. Dimorogonas, A.D., Dynamic response of cracked rotors. General Electric Co., Internal report, Schenectady, NY, U.S.A., 1971.
7. Dimorogonas, A.D., Dynamics of cracked shafts, General Electric Co., Technical information Series. DF-74-LS-79, 1974.
8. Matveev, V.V. and Bovsunovsky, A.P., Vibration based diagnostics of fatigue damage of beam-like structures, Journal of Sound and vibration, 249(1), 2002, pp.23-40.
9. Adams, R.D., Cawley, P., Pye, C.J. and stone, B.J., A vibration technique for non-destructively assessing the integrity of structures. Journal of Mechanical Engineering Science., 1978.
10. Springer, W.T., Lawrence, k.L. and Lawley, T.J., The effect of a symmetric discontinuity on adjascent material in a longitudinally vibrating uniform beam. Experimental Mechanics, 1987, 27, pp. 168-171.
11. Krawczuk, M. and Ostachowicz, W.M., Parametric vibrations of beam with crack. Ing.Arch., 1992, 62,463-473.
12. [12].Krawczuk, M.natural vibration of cracked rotating beams. Acta Mechanica, 1993, 99, pp.35-48.

13. Silva, J.M.M. and Gomez, A.J.M.A.m Experimental dynamic analysis of cracked free-free beams. Exp. Mech., 1990, 30, pp.20-25.
14. Araujo Gomez, A.J.M. and Montalvaoe Silva, J.M., Theoretical and Experimental data on crack depth effects in the dynamic behaviour of free-free beams. Int. Modal Analysis Conference, IMAC, Vol.9. Union Coll, Schenectady, NY,U.S.A., 1991, pp. 274-283.
15. Araujo Gomez, A.J.M. and Montalvaoe Silva, J.M., Experimental determination of the influence of the cross-section size in the dynamic behaviour of cracked beams. Proc. IMMDC2, Los Angels, U.S.A., 1990, pp.124-130.
16. Chondros T.G, Dimarogonas A.D and Yao, J., A continuos cracked beam vibration theory. Journal of Sound and Vibration, Vol.215, 1998, pp.17-34.
17. Papadopoulos, C.A., Torsional vibrations of rotors with transverse surface cracks,. Computers and Structures Vol.51, No.6, 1994, pp.713-718.
18. Pandey.A.K, Biswas, m. and Samman, M.M., Damage detection from changes in curvature mode shapes. Journal of Sound and vibration, 1991, 145, pp. 321-332.
19. Qian, G.-L., Gu, S.-N. and Jian J.-S., The dynamic bahaviour and crack detection of a beam with a crack. Journal of Sound and Vibration, 1990, 138(2), pp.233-243.
20. Zheng, D.Y. and Fan, S.C., Natural frequencies of a non-uniform beam with multiple cracks via modified Fourier series. Journal of Sound and Vibration, Vol.242 (4), 2001, pp. 701-717.
21. Timoshenko, S.P. and Gere, J.M., Theory of Elastic Stability, 2nd edn. McGraw-Hill, New York (1961).
22. Wang, T.M, Postbuckling of column under distributed axial load. J.engg Mech. 97. 1323 (1971).
23. Wang, C.Y, Large deformation of a heavy cantilever. Q. appl. Math. 39, 261, (1981).
24. Wang.C.Y, A critical review of the heavy elastica. International Journal of Mechanical Sciences. 28, 549 (1986).
25. Tauchert, T.R and W.Y.Lu, W.Y, Large deformation and postbuckling behavior of an initially deformed rod. Int. J. Non-Linear Mech. 22,511 (1987).

26. Wilson, J.F and Snyder, J.M, The elastica with end load flip-over. Journal of Applied Mechanics. 55, 845 (1988).
27. Dimarogonas, A.D., and Papadopoulos, C.A., "Vibration of cracked shaft in bending", Journal of Sound and Vibration, 1983, **91**, 583-593.
28. Chondros, T.G., and Dimarogonas, A.D., "Identification of cracks in welded joints of complex structures, Journal of Sound and Vibration, 1980, **69**, 531-538.
29. Dimarogonas, A.D., and Massouros, G., "Torsional vibration of a shaft with circumferential crack", Engineering Fracture Mechanics, 1980, **15**, 439 – 444.
30. Rizos, P.F., Aspragathos, N., and Dimarogonas, A.D., "Identification of cracked location and magnitude in a cantilever beam from the vibrational modes", Journal of Sound and Vibration, 1989, **138** (3), 381 – 388.
31. Mermertas, V., and Erol, H., "Effect of mass attachment on the free vibration of cracked beams", The 8th International Congress on Sound and Vibration, Hong Kong, , 2001, 2803 – 2810.
32. Bamnios, G., and Trochides, A., "Dynamic behavior of cracked cantilever beam", Applied Aoustics, 1995, 97 – 112.
33. Dimarogonas, A.D., "Vibration of cracked structures: a state of art review", Engineering Fracture Mechanics, 1996, **55**, 831 – 857.
34. Chandra Kishen, J.M., and Kumar, A., "Finite element analysis for fracture behavior of cracked beam-columns", Finite Elements in Analysis and Design, 2004, 40, 1773 –1789.
35. Krawczuk, M., Zak, A., and Ostachowicz, W., "Elastic beam finite element with a transverse elasto-plastic crack", Finite Elements in Analysis and Design, 2000, 34, 61 – 73.
36. .Ostachowicz W.M., and Krawezuk, M., "Analysis of effect of cracks on the natural frequencies of a cantilever beam", Journal of sound and vibration, 1991, 150(2),pp.19-201.
37. Behera, R.K., "Vibration of a cracked cantilever beam", M.E.Thesis
38. Parhi, D.R.K., "Dynamic behavior of beam/rotor -structures with transverse crack subjected to external force", PhD thesis.